WYLE LABORATORIES - RESEARCH STAFF

REPORT WR 66 - 40

FATIGUE OF REINFORCED CONCRETE DUE TO SINUSOIDAL AND RANDOM LOADINGS

by

G.C. Chan

Work Performed Under Contract No. NAS 8 - 5384

Prepared by G.C. Chan
G.C. Chan

Approved by
Kenneth McK. Eldred
Director of Research

Date July 1966

1

COPY NO. _____

SUMMARY

11684

This report describes an experiment of reinforced concrete beams under dynamic loadings. Specially designed scale beams were vibrated with sinusoidal and random inputs to the foundations. These beams were 1.5" x 3.5" x 25" in size. The coarse aggregates - fine aggregates and the reinforcing steel were carefully scaled in order to simulate an ordinary reinforced concrete structure. Load-cycle curves for forty seven beams under sinusoidal tests and twenty one beams under random tests were measured. A few light weight, lightly reinforced beams cut from commercial roof slabs were also tested. A literature survey of the state-of-the-art of reinforced concrete and its fatigue properties was also included. AUTHOR

TABLE OF CONTENTS

LIST OF TABLES

LIST OF FIGURES

LIST OF FIGURES (Continued)

LIST OF SYMBOLS

a	height of a WF channel
A	cross-sectional area
c	distance from neutral axis to outermost fiber of a beam
E	Young's modulus of elasticity
f	frequency, cps
$\mathcal{F}$	generalized force
g	acceleration, unit in g
g	gravitational acceleration, 386 in/sec^2
G_{ult}	as defined in page 13
H	dynamic magnification factor
i	$= \sqrt{-1}$
I	area moment of inertia
k	spring constant
L	length of beam between supports
m	mass
M_o	total mass of beam
M	bending moment
$\mathcal{M}$	generalized mass
n	subscript for modal number
N	total cycles of vibration
P	static failing load
Q	dynamic magnification factor at resonance
S, σ	stress
S	power spectral density, g^2/cps
t	time
U	foundation deflection
W, y	relative beam deflection of beam

LIST OF SYMBOLS (Continued)

x	beamwise coordinate
Y	absolute deflection of beam
ρ	density
ζ	damping ratio = $1/2\,Q$
μ	mass per unit length
ϕ	mode shape
ω	frequency, rad./sec.
η	loss factor $\cong$ $1/Q$

1.0 INTRODUCTION

The trend in today's missile and rocket technology is toward bigger and more powerful vehicles. As a result of this upward trend, any building, either governmental at the launch site or the static firing pads, or residential, some distance away from these sites may frequently be subjected to high intensity sound. Undoubtedly, the safety of such buildings in the areas of intense noise and vibration is of great interest to many engineers and designers. Some of the most commonly used construction materials are plain and reinforced concrete. Therefore, a better knowledge of the dynamic properties of concrete is necessary in the design of buildings where material fatigue or severe vibration are encountered.

The purpose of the experiment to be described in this report is to obtain useful data on reinforced concrete subjected to sinusoidal and random dynamic loadings. Approximately one hundred fabricated reinforced concrete beams were tested. Fifteen percent of these beams were tested statically to determine their static strength. The remaining beams were tested to determine their dynamic fatigue characteristics. The beams were mounted, one at a time, on an electromagnetic shaker and were vibrated at their supports. Desired stress levels were maintained by monitoring the input signal to the shaker. The number of vibration cycles was established up to the moment of the specimen's failure. The reinforcing wires imbedded in the concrete beams were also tested by a tensile machine to determine their yield and ultimate tensile strength, and to give a better understanding of the strength of the reinforced concrete specimen analytically. Some light weight commercial roof slabs were also tested.

2.0 TECHNICAL DISCUSSION

Before the experimental work began, a literature survey was conducted to investigate the properties of concrete, and in particular, reinforced concrete. The survey covered most work performed in the United States and abroad spanning roughly the past century. This survey shows:

(1) Random loading of concrete has not been investigated.

(2) Very little work has been performed on concrete subjected to high speed, dynamic and complete reversal load.

(3) Most tests conducted up to date were of low speed, zero-to-maximum loading type. The test specimens were tensile reinforced only at one side. Test data were occasionally extended for complete reversal load situations beyond the range of experimental supports.

(4) From the existing data on low speed, zero-to-maximum load tests, the following conclusions can be made:

For plain concrete -

(i) Ultimate compressive strength of the commonly used concrete is between 3,500 to 5,000 psi. The ultimate tensile strength is between 400 and 500 psi.

(ii) The endurance limit is 50 to 55 percent of the ultimate strength at 10^6 load cycles. However, it is doubtful that plain concrete possesses an endurance limit at least within 10^7 load cycles.

(iii) Plain concrete fails in tension for reverse cycle loading.

(iv) The S-N curve for plain concrete, zero-to-maximum load is shown in Figure 1.

For reinforced concrete -

(i) Reinforced concrete may fail in bondage, shear (diagonal tension), flexural compression, or fatigue of the reinforcement.

(ii) Cracks in reinforced concrete do not always result in rapid failure.

(iii) The endurance limit of reinforced concrete, subjected to zero-to-maximum loading, can be assumed to be 50 to 55 percent of the static ultimate strength. However, some tests indicate that 40 percent should be used for a specimen which is weak in shear.

(iv) The dynamic ultimate strength is found some 30 to 40 percent higher than the static ultimate strength, depending on the size and length of the specimens.

(v) The dynamic magnification factor, Q, (defined as the equivalent of the inverse of twice the damping ratio) is between 6 and 8.5.

(vi) The rate of repeated loading at a rate much below resonance frequency appears to have no effect in the fatigue strength. However, a very slow rate, for example, 10 cycles per minute, seems to decrease the fatigue strength. A period of rest between repeated loadings tends to restore strength.

(vii) The S-N curve for reinforced concrete, (one to two percent reinforcement), with zero-to-maximum load is shown in Figure 2.

(5) Laboratory test data on fatigue properties may serve as a guideline in structural design. However, adverse corrosive conditions in service could easily reduce the fatigue strength.

(6) The stress-strain relationship of concrete is not quite linear. The stress-strain curve may be slightly concave or convex in nature, depending on the specimen's previous load-cycle history. The dynamic Young's modulus of elasticity is slightly higher than that for the static case. In the case of very fast rate of loading, such as in a wave propagation experiment, a distinct increase, of the order of 25 percent, was reported in the magnitude of the dynamic Young's modulus relative to its static value.

(7) The elasto-plastic nature and the nonlinear behavior of concrete make resonant frequency fatigue tests difficult.

This literature survey indicates that there exists a severe lack of work in the field of dynamic properties of reinforced concrete structure.

From the literature survey and from elementary engineering considerations, we observe that concrete is made of heterogeneous materials and is visco-elastic in nature. The static strength is influenced by a number of factors such as, aggregate sizes, qualities of sand and stones, age, initial concrete mix, curing, corrosion, and local stress concentration. In the dynamic testing, a concrete specimen is also greatly affected by cracks, increase of internal damping, variations in Young's modulus, and change in effective cross-sectional area of the specimen. Undoubtedly, it is not an easy task to estimate the true dynamic and the true static strength of a concrete specimen.

On the other hand, if the true values of the static and dynamic strengths were obtained, they may not be directly applicable to ordinary structural design calculations, where only simple stress-strain and stress-moment equations are available. Because of this reasoning, the experiment to be described in this report will minimize the complicated nature of concrete under both static and dynamic tests in order to use the simple

stress-strain and stress-moment relationships in the estimation of stress, moment, and life cycles.

The reinforced concrete is, therefore, assumed homogeneous, isotropic, and to have a Young's modulus of 2.5×10^6 psi (2.0×10^6 psi for plain concrete) regardless of its previous vibration history. Small cracks usually result in a change of bending stiffeners, EI, which, in turn, accounts for the lowering of the resonance frequency. Cracks also increase the internal damping, which affect the resonant dynamic magnification factor, Q, and therefore, the specimen response to excitation. All stress, strain, resonant frequency, and bending moment calculations are made under the assumption that the concrete specimen is intact and without cracks. However, small cracks during a dynamic test do not mean failure. The criterion of failure in the experiment to be described is arbitrarily defined when one or more of the following conditions is obtained.

(i) Complete failure of the specimen - specimen breaks into two halves.

(ii) Complete failure of steel reinforcement.

(iii) Severe damage results in changing of bending stiffeners, E I, and decreasing of the resonant frequency. A specimen is considered to have failed when the resonant frequency is reduced to half of its initial value.

(iv) Significant amounts of broken concrete pieces fall from specimen.

3.0 TEST SPECIMENS

Two groups of test specimens were available for this experiment.

Group (1): Forty five 3" x 1" x 25" reinforced concrete beams were cut from three 24"x 1" x 76" light weight concrete roof slabs, manufactured by the Alabama Cement Tile Company. The slab manufacturer provided the following specifications:

Trade name: Alaslab
Density: 12 lb/sq.ft.
Allowable load: 60 lb/sq.ft.
Age: More than 90 days
Reinforcement: 4 x 4 - 14 gage welded mesh fabric at center of slab; not rusty.
Aggregate: Light weight; high limestone component; maximum size not greater than 3/8"

Group (2): One hundred and thirty, 3-1/2" x 1-1/2" x 25", 2.52 percent reinforced concrete scale model beams were manufactured specifically for this experiment. The following cross-sectional diagram shows the dimensions of these beams.

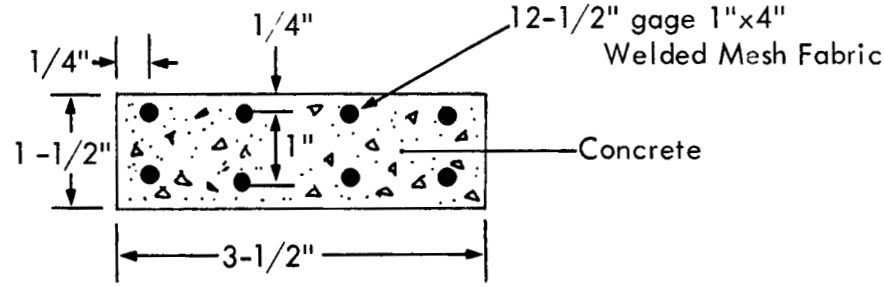

Cross-Section of a Scale Model Beam

The table below gives a comparison of the scale model beam to a 6 inch reinforced concrete beam of typical construction:

	6" Typical Beam	Scale Model Beam
Scale Factor	1	1/4
Thickness of Beam	6"	1-1/2"
Steel Diameter	3/8" (0.38")	12-1/2 gage (0.1")
Steel	Deformed Bar	Smooth, Welded Mesh Fabric
% of Reinforcement	0.5 to 2.5%	2.52%
Coarse aggregate	#4 to 1" Screen	# 16 to 3/8" Screen
Fine Aggregate	# 100 to #4 Screen	#200 to #16 Screen
Mixed Ratio	1 : 1 : 2 to 1 : 1-1/2 : 3	1 : 1 : 2
Water gal./sack of cement	5	5.5
Slump Test	3" to 6"	7" to 8"‡
Distance, Center of Steel to Concrete Surface	1" to 1-1/2"	1/4"
Cylinder Compression Test:		
(7 days)	2000 - 3000 psi	2730 psi*
(28 days)	4000 - 5000 psi	4770 psi*
Cement	Portland, Type I	Portland, Type I
Curing Conditions	In Air	In Air

*Average of 5 cylinders. Test performed by Barrow-Agee Laboratories, Inc. Huntsville.

‡Actual concrete mixing.

It should be noted that the material strength used in the model beams was in the compatible range of that of the ordinary concrete work. The scale model beams used in the sinusoidal tests were cured two to four months. These beams used in the random tests were cured six months or longer.

The aggregate composition of the scale model beams is shown in the following histogram. The aggregate composition of a typical 1 : 1 : 2 mixed reinforced concrete beam of six inch thickness is also shown for comparison:

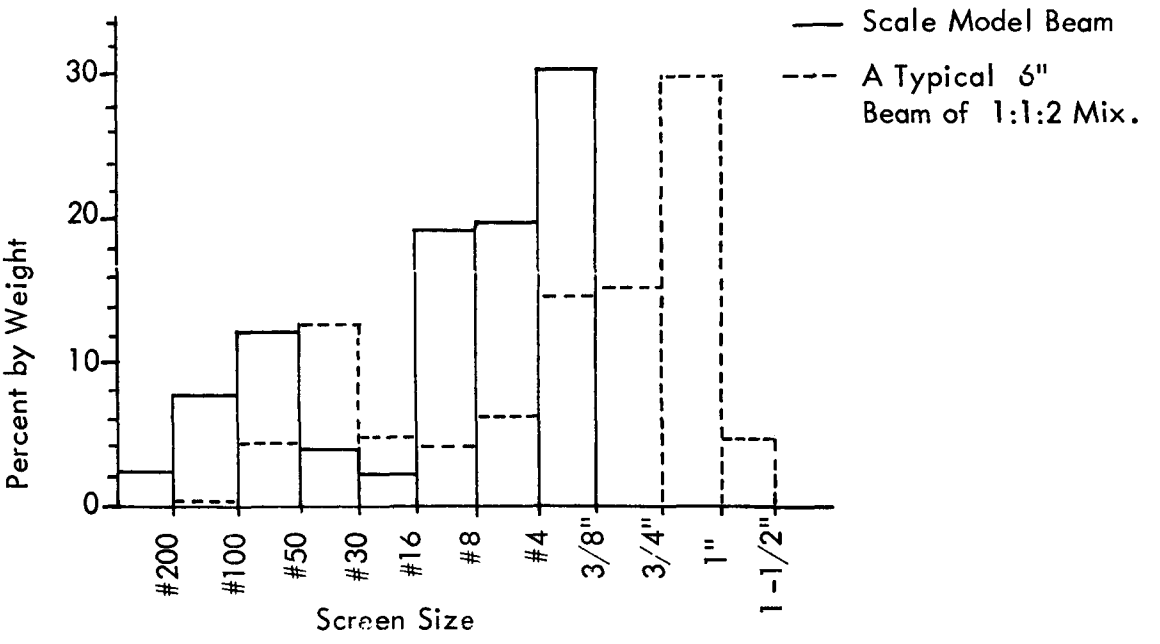

Comparison of Aggregate Compositions of Scale Model Concrete Beam with a Typical 1 : 1 : 2 Mixed 6" Thick Beam

The calculations of the moment of inertia of the tensile reinforced concrete beam and its natural frequency are presented in Appendix A.

Approximately 20 percent of the beams belonging to the group (1) category were found defective due to initial cracks, cutting fault, and mishandling. Seven of the good specimens were tested statically. The ultimate strength was established at maximum static failing load. The remainder of the group (1) beams were tested dynamically with sinusoidal excitation at the excitation frequency adjusted close to, but less than the resonant frequency of the specimen. A large proportion of these beams were used to perfect this dynamic testing technique. Only a small number of these beams yielded meaningful results.

A few of the scale model beams in the group (2) category were discarded due to faults attributed to the manufacturing process. Eight of the good specimens were chosen randomly and were tested statically to establish the ultimate static strength. Forty six beams were tested dynamically with sinusoidal input to the beam supports. Twenty one beams were tested with random signal input.

4.0 TEST METHODS

In both the static and dynamic tests, a concrete beam specimen was simply supported at both ends, 23.5 inches apart. The static ultimate bending strength of the concrete beam was determined by the four point static loading method as shown in Figures 3 and 4. This method employed a five inch WF channel at the middle of the beam causing the beam to fail, by static loading on the channel, at a section of uniform bending moment. The modulus of rupture is the calculated stress by the following familiar formula:

$$\text{Stress} = Mc/I$$

where M = bending moment at failing load

$$= \frac{P}{4}(L - a)$$

P = static failing load

L = length of beam between supports

a = height of the WF channel

I = moment of inertia

c = distance from outermost fiber to the neutral axis .

The dynamic strength was determined, on the other hand, by vibrating the beams at their two end supports. The tests consisted of sinusoidal input and random input to the electromagnetic shaker (MB model C-25-H) which vibrated the beam supports. The test setup and the associated equipment used are shown in Figures 5, 6, and 7.

In both static and dynamic tests, the concrete beam specimens were simply supported at both ends 23-1/2 inches apart. Metal film strain gages (Budd Company type C6-161) were used to measure strain of the beam in the early stages of dynamic testing. Small pieces of steel shim stock , 0.003 inch thick, were first attached to the concrete surface by an epoxy cement. The strain gages were then cemented to the shim stock. However, this method of determining strain was found to be very erratic. The strain measurement was easily effected by local cracks in neighborhood of the strain gage.

A second method of estimating the desired stress level was developed on the basis of relative acceleration. Appendix B shows that, for a pinned-pinned beam with moving supports, the fundamental mode shape, relative to the supports, is essentially a half sine wave, the same as for fixed supports, with sinusoidally distributed load applied throughout the entire beam length. The maximum stress at the outermost fiber of a beam specimen is a function of the applied bending moment. This bending moment is in turn a function of acceleration, frequency, and mode shape. It is, therefore, possible to control the desired stress at any point of the beam by carefully

monitoring the input to the shaker. This second method of stress control was used throughout the rest of the test program.

In the sinusoidal dynamic test, the input to the shaker was adjusted continuously so that a constant relative displacement at the middle of the beam was maintained until the beam failed. The excitation frequency was monitored to be about 5 to 10 percent higher than the beam resonant frequency. The continuous input adjustment was necessary since the resonant frequency was falling quite rapidly as a result of cracks and change in bending stiffeners. The peak stress at the maximum strained location - that is, at the middle of the beam, was computed from the controlled relative acceleration, and was normalized by the modulus of rupture from the static test, to give the load ratio. This ratio, together with the excitation frequency and the total time of run, constituted a point in the load-cycle, (S-N), curve of the concrete specimen.

However, in the random input dynamic test, the control of constant stress at mid-span of the beam was achieved in a different way. Instead, a broad band, 20-220 cycles, flat spectrum of input was held constant throughout a test run. The relative acceleration response of the specimen was analyzed by passing the signal through a power spectral density analyzer with a narrow (20 cycles) variable center frequency band pass filter. The spectral density of response and the center frequency of the filter were recorded sinultaneously on a dual channel visicorder. The peak value of the acceleration response, g_{peak}, at the onset of the test was normalized by a factor G_{ult}. This factor is the hypothetical sinusoidal acceleration that would cause a maximum bending moment to be applied to the beam, at the beam's resonance frequency, exactly large enough to induce failure at the first half of a vibration cycle. This ratio, g_{peak}/G_{ult}, the resonant frequencies, and the total time required to fail a specimen constituted a point, again, in the load-cycle curve. (For further details, see the following section.)

The ultimate tensile strength of the reinforcing wire was determined by an axial pulling machine. The stress-strain curves of several wires are presented in Figure 8. The ultimate tensile strength is calculated to be 68,000 psi. Figures 9 through 12 show some typical test records of the concrete beams during sinusoidal dynamic tests. Figures 13 through 16 are a few examples of the beam data under random dynamic tests. The filter center frequency and the beam's relative response were recorded simultaneously for the random dynamic tests in order to estimate the value of the resonant frequency. Figures 17 and 18 are typical response records of a beam, at low level scans for different numbers of accumulated vibration cycles. Comparison of these two figures indicates the magnitude change of resonance response of a beam.

5.0 CALCULATION OF STRESSES

The calculation of stresses in the group (1) and group (2) test specimens, subjected to sinusoidal foundation excitation, are the same. Therefore, only those of group (2) will be presented in greater detail in this section.

Group (2) Specimens, Sinusoidal Test:

From Section 6.0, the average failing static load was 585 lbs.

Maximum bending moment, $M_{max} = \frac{P}{4}(L - a)$

$= 2850$ in.-lb.

Maximum Stress, $\sigma_{max} = \frac{M_{max} c}{I}$

$= 5650$ psi .

However, since relative acceleration of the beam specimen was being controlled in the dynamic test, the ultimate strength of the specimen could be expressed in a more convenient form as the acceleration, G_{ult}; i.e., the hypothetical acceleration, which would produce a bending moment of 2850 in. - lb. at the first half cycle of vibration.

The theory of vibration of a simply supported beam with a moving foundation is presented in Appendix B. It is shown in this appendix that the realtive fundamental mode shape (that is, the absolute mode shape of the beam with respect to the motion of the support) is essentially a half-sine wave. Since the excitation frequency of the beam is either discrete in nature, as in the case of sinusoidal test, or of a limited band width, as in the random testing case, and since the even mode of vibration is suppressed as shown in Appendix B, the fundamental mode is the predominant mode in response vibration, and is the most important mode in the stress analysis. We have, therefore, the following expression for the relative mode shape:

$$y(x,t) = y_c \sin \pi \frac{x}{L} \cdot e^{i\omega t} \quad \text{(pinned-pinned beam)}$$

where y_c = maximum deflection of beam

x = spanwise coordinate

L = length of beam

ω = excitation frequency $= 2\pi f$

t = time .

$$\text{Thus} \quad \ddot{y}(x,t) = \frac{\partial^2 y(x,t)}{\partial t^2} = -\omega^2 y_c \sin \pi \frac{x}{L} e^{i\omega t}$$

$$= -\omega^2 y(x,t)$$

$$\text{or} \quad y(x,t) = -\frac{1}{\omega^2} \ddot{y}(x,t) \cdot$$

The maximum bending moment occurs at $x = \frac{L}{2}$, and is

$$M_{max} = E I \left| \frac{\partial^2 y(x,t)}{\partial x^2} \right|_{max}$$

$$= E I \left(\frac{\pi}{L}\right)^2 y(x,t)_{max}$$

$$= E I \left(\frac{\pi}{L}\right)^2 \frac{\ddot{y}(x,t)_{max}}{\omega^2}$$

$$= E I \ddot{y}(x,t)_{max} \left(\frac{1}{2fL}\right)^2 ,$$

$$\text{or} \quad \ddot{y}(x,t)_{max} = \frac{4 f^2 L^2}{E I} M_{max} \quad \text{(For pinned-pinned end fixity)}$$

For a sinusoidal test, the frequency, f , in the above equation is the excitation frequency. However, in the random test, f is the resonant frequency of the beam specimen.

To express the ultimate strength of the concrete beam in terms of acceleration, we assume that the static stress-strain relationship and that for the dynamic case are the same for the test specimen, and that $y(x,t)_{max}$ must equal G_{ult}, a hypothetical static equivalent acceleration which would produce the required bending moment, M_{max}, of 2850 in. - lb. at the end of the first half cycle of vibration. And, for the given beam specimen of:

$$L = 23.5 \text{ inches}$$
$$E = 2.5 \times 10^6 \text{ psi}$$
$$I = 0.426 \text{ in.}^4 .$$

The value of G_{ult} is calculated as

$$G_{ult} = \frac{4 \times f^2 \times (23.5)^2}{2.5 \times 10^6 \times 0.426} \quad 2850 \times \frac{1}{386}$$

$$= 1.53 \times 10^{-2} \times f^2 \quad g^*_{peak} .$$

At the excitation frequencies of 80, 90, and 100 cps:

$$G_{ult} = 98 \; g_{peak} \text{ at } 80 \text{ cps}$$
$$= 124 \; g_{peak} \text{ at } 90 \text{ cps}$$
$$= 153 \; g_{peak} \text{ at } 100 \text{ cps}.$$

For group (1) specimens:

$$G_{ult} = 4.24 \times 10^{-3} \times f^2 \; g_{peak}$$

---

*1 g unit = 386.4 in./sec.^{2} Acceleration.

or $G_{ult} = 27.1\ g_{peak}$ at 80 cps

$= 34.4\ g_{peak}$ at 90 cps

$= 42.4\ g_{peak}$ at 100 cps.

The following table gives the percent of load (dynamic load/static load) and the required acceleration for various frequencies for the group (2) specimens under a sinusoidal dynamic test.

TABLE I

Required Relative Acceleration in (g peak) for Various Percentages of Loads and Excitation Frequencies.

(Based on the Equation $G_{ult,\ 100\%} = 1.53 \times 10^{-2} \times f^2\ g_{peak}$)

% Load \ f cps	110	105	100	95	90	85	80	75	70	65	60	55	50
115						126	113	99	86	75	63	53	44
110					136	122	108	95	82.5	71.5	60.5	50.5	42
105				145	130	106	103	90.5	79	68	58	48	40
100			153	138	124	111	98	86	75	65	55	46	38
95		153	145	131	118	105	93	82	71	62	52	44	36
90	166	145	138	124	112	100	88	77.5	67.5	58.5	49.5	41	34
85	157	137	130	117	105	94	83	73	64	55	47	39	32
80	148	129	122	110	99	88.5	78	69	60	52	44	37	30
75	139	121	115	103	93	83	73.5	64.5	55	48	41	35	28.5
70	130	113	107	97	87	77.5	68.5	60	52.5	45.5	38.5	32	26.5
65	120	105	99.5	90	81	72	64	55	49	42	36	30	25
60	110	96.5	92	83	74.5	66.5	59	52	45	39	33	28	23
55	102	88.5	84	76	68	61	54	47	41	36	30	25	21
50	92.5	80.5	76.5	69	62	55.5	49	43	38.5	32.5	27.5	23	19

In terms of stress, $G_{ult} = 4 f_1^2 L^2 \sigma_{ult}/E c g$ for pinned-pinned beam, and it can be shown, see example 2 of Appendix C, that for clamped-clamped beam, $G_{ult} = f_1^2 L^2 \sigma_{ult}/E c g$.

The dynamic response of a concrete beam specimen under broad band random excitation is to be calculated next. The following assumptions are to be noted:

(1) Euler's equation for beam is used with negligible effects of rotary inertia and shear deformation.

(2) Small deflection theory applied.

(3) Pinned-pinned end flexity.

(4) Input spectrum is flat within a bandwidth of 20 - 220 cycles and zero elsewhere.

(5) Only the fundamental mode of vibration is important. Higher modes are neglected.

(6) The dynamic magnification factor $H(\omega)$ is defined as

$$H(\omega) = \frac{1}{\sqrt{\left[1 - \left(\frac{\omega}{\omega_n}\right)^2\right]^2 - \left(2\zeta\frac{\omega}{\omega_n}\right)^2}}$$

where ζ is the damping ratio,

ω_n = natural frequency.

And at resonance, i.e., $\omega = \omega_n$;

$$H(\omega) = Q = \frac{1}{2\zeta}$$

Q is also a function of damping ratio ζ only.

(7) Since the resonant frequency is more affected by bending stiffness variations than variations in damping, the big drop in resonant frequency is mainly due to the continuous change of bending stiffeners, EI, as the beam specimen cracks under severe vibration.

Considering only the fundamental mode, we have, for the beam response:

$$W_1(\omega) = \frac{\mathcal{F}_1}{\mathcal{K}_1} Q = \frac{\mathcal{F}_1 Q}{m_1 \omega_1^2}$$

where $\mathcal{F}$ = the generalized force

$\mathcal{K}$ = the generalized spring constant

$\mathcal{M}$ = the generalized mass

ω_1 = fundamental natural frequency

W = deflection response at midspan of beam

1 = subscript for fundamental mode.

The generalized force can be expressed as

$$\mathcal{F}_1 = \ddot{W}_o \int_o^L \phi(x)\, dm$$

$$= \ddot{W}_o \frac{\mu L}{\pi} \int_o^1 \sin \frac{\pi x}{L}\, d\pi \frac{x}{L}, \text{ pinned-pinned beam}$$

$$= 2 \frac{M_o}{\pi} \ddot{W}_o$$

where L = length of beam

ϕ = mode shape of beam

μ = mass per unit length of beam

M_o = total mass of beam .

The generalized mass $\mathcal{M}_1$ is $\frac{1}{2} M_o$.

Substituting $\mathcal{F}_1$ and $\mathcal{M}_1$ into equation of $W_1(\omega)$ and differentiating twice with time, we get the response acceleration :

$$\ddot{W}_1(\omega) = \frac{4}{\pi} \ddot{W}_o Q \frac{\omega^2}{\omega_1^2}$$

where $\ddot{W}_o$ is the foundation acceleration.

The mean square response for the first resonant frequency is:

$$\overline{\ddot{W}_1^2(\omega_1)} = \left(\frac{4}{\pi}\right)^2 Q^2 \overline{\ddot{W}_o^2}$$

or

$$\left(\frac{\overline{\ddot{W}_1^2(\omega_1)}}{\Delta f}\right) = \left(\frac{4}{\pi}\right)^2 Q^2 \left(\frac{\overline{\ddot{W}_o^2}}{\Delta f}\right)$$

$$S_{\ddot{W}_1}(\omega_1) = \frac{16}{\pi^2} Q^2 S_{\ddot{W}_o}(\omega_1)$$

$$\cong 1.6\ Q^2\ S_{\ddot{W}_o}(\omega_1)$$

$$\frac{S_{\ddot{W}_1}(\omega_1)}{(Q)^2} \cong 1.6\ S_{\ddot{W}_o}(\omega_1)$$

where Δf = frequency band

$S_{\ddot{W}_1}(\omega_1)$ = resonant response power spectral density, g^2/cps

$S_{\ddot{W}_o}(\omega_1)$ = input power spectral density, g^2/cps .

The rms acceleration response can be expressed as:

$$g_{rms} = \left[\frac{\pi}{2}\ S_{\ddot{W}}(\omega_1)\ \frac{f_1}{Q}\right]^{1/2}$$

$$= \left[\frac{\pi}{2}\ 1.6\,Q^2\ S_{\ddot{W}_o}(\omega_1)\ \frac{f_1}{Q}\right]^{1/2}$$

$$= 1.58\left[S_{\ddot{W}_o}(\omega_1)\ Q\ f_1\right]^{1/2} .$$

The rms response of a simple structure to a narrow-band random excitation of a known rms level is equivalent to the response produced by sinusoidal excitation of the same rms level. If it is assumed that the peak-to-rms value of the stress time history is 3, the use of a sinusoidal excitation that has a peak amplitude equal to three times the rms value of the random excitation should cause no failures that would not be caused by the random excitation. Thus, the equivalent sinusoidal peak acceleration can be expressed as:

$$g_{peak} = 3\left[1.58^2 S_{\ddot{W}_o}(\omega_1)\ Q\ f_1\right]^{1/2}$$

$$= 4.75\left[S_{\ddot{W}_o}(\omega_1)\ Q\ f\right]^{1/2}.$$

For an intact beam specimen at the onset of a random vibration test, $f_1 = 81$, $Q = 8$, we have

$$g_{peak} = 121\left[S_{\ddot{W}_o}(\omega_1)\right]^{1/2}.$$

The following table, calculates the g_{peak} by the above equation, for various input conditions. The inputs are in rms accelerations.

TABLE 2

Calculations of Response Power Spectral Density $S_{\ddot{W}_1}(\omega_1)$ and Ratio of g_{peak}/G_{ult} for Various Random Inputs.

Input RMS Accel. g	g^2	$S_{\ddot{W}_o}(\omega_1)$† g^2/cps	$\sqrt{S_{\ddot{W}_o}(\omega_1)}$	$S_{\ddot{W}_1}(\omega_1)$ g^2/cps	Peak Response‡ Accel. g	$\frac{g_{peak}}{G_{ult}}$*
2.0	4	0.02	0.141	2.05	17.1	0.17
3.0	9	0.045	0.212	4.61	25.7	0.26
4.0	16	0.08	0.283	8.20	34.3	0.34
6.0	36	0.18	0.415	18.45	50.2	0.50
8.0	64	0.32	0.565	32.80	68.4	0.68
10.0	100	0.50	0.707	52.25	85.6	0.85
12.0	144	0.72	0.847	73.80	102.6	1.02

† For flat spectrum between 20 to 220 cps,

$$S_{\ddot{W}_o}(\omega_1) = \frac{g^2}{200} .$$

‡ For virgin specimen, f = 81 cps, Q = 8.

* $G_{ult} = 100.3\ g_{peak}$ from previous calculations.

Figure 19 shows a pair of typical input and response power spectral density curves taken directly from test beam No. 84. The acceleration signals were recorded on tapes simultaneously and were processed through an analyzer at a later date.

6.0 INSTRUMENTATION

The instrumentation used for the performance of the tests is listed below:

(1) Bruel and Kjaer (B and K) Automatic Vibration Exciter Control, Model 1019.

(2) MB Electromagnetic Shaker, Model C25H, Type A, MB Mfg. Co.

(3) Ling Electromagnetic Shaker, Model 249.

(4) Electronic Frequency Counter, Hewlett and Packard Model 521 A R.

(5) Wyle 10KW Power Amplifier.

(6) Ling Power Amplifier, PP 120-150.

(7) Honeywell Visicorders, Models 1508 and 1012.

(8) Oscilloscope, Tektronix Inc. Type 545A.

(9) Strain Gage Indicator, Strainsert Co. Model HW 1.

(10) Endevco Accelerometers, Models 2213 c and 2226.

(11) Spectral Dynamics Corp. Constant Output Level Adapter, Model SD 11.

(12) Ling Automatic Spectral Density Equalizer and Analyzer, Model 80.

(13) Consolidated Electrodynamics Corp. Tape Recorder, Model GR 2800.

(14) Spectral Dynamics Corp. Tracking Filters, Model SD 101.

(15) Mosley Log Converters, Model 60D.

(16) Endevco Charge Amplifiers, Model 2711.

(17) Electro Instrument Differential Amplifier, Model A 20B-2.

In each of the dynamic tests of the scale concrete beams, four accelerometers were employed. The first accelerometer was cemented to the shaker table and was used to check that the shaker was within its force limitation. The second accelerometer was cemented at the middle and on the top surface of the beam. The third accelerometer was cemented to the concrete specimen exactly at one of the pinned end supports. The accelerometer signals of the second and third accelerometers were fed into a differential amplifier to give the relative acceleration at midspan with respect to the support. A fourth accelerometer was cemented close to the second accelerometer to give the absolute acceleration at midspan. Typical experimental accelerations are presented in Figure 12. In some tests, the accelerations from the third or the fourth accelerometers were not recorded. It was noticed that for this accelerometer arrangement, the accelerations from the first and third accelerometers were not identical, and that the first accelerometer should not be used in place of the third to give, together with the second accelerometer, the relative acceleration.

7.0 TEST RESULTS

The following tables summarize the results of various tests:

Table No.	Contents of Table
3	Static tests of group (1) specimens (commercially fabricated roof slabs).
4	Dynamic tests of group (1) specimens, with sinusoidal input to the shaker.
5	Static tests of group (2) specimens (scale reinforced concrete beams).
6	Dynamic tests of group (2) specimens, with sinusoidal input to the shaker.
7	Dynamic tests of group (2) speciments, with random input to the shaker.
8	Test data sheet evaluated from a typical test record such as shown in Figure 13.

Figure 20 shows the plot of the stress-cycles (S-N) curve from data of Tables 1 and 2. Figure 21 shows the S-N curve of the scale model beams under dynamic sinusoidal loads. Figure 22 shows the same model beams under dynamic random loads. Figure 23 shows the drops in resonance frequency and resonance dynamic magnification factor, Q, as a function of cycles of vibration for a typical beam under random excitation.

TABLE 3

Static Tests of Group (1) Specimens (Commercially Fabricated Roof Slabs)

RUN NO.	P, FAILING LOAD, lbs.*
1	79
2	88
3	79
4	94
5	75
6	101
7	96
	87.4 Average

* ±2 lbs. Estimated error

Moment at Static Failure, $M_{max} = \frac{P}{4}(L - a)$

$= 402$ in. - lb.

Maximum Stress, $\sigma_{max} = \frac{M_{max}\, c}{I}$

$= 730$ psi (Bending) .

TABLE 4

Dynamic Test of Group (1) Specimens, with Sinusoidal Input.

Excitation frequency was about 10% lower than the specimen resonant frequency.

Run No.	Freq. cps.	Accel. g's	%Modulus† of Rupture	Time† sec.	No. of Cycles* at Rupture
27	100	27.5	65	120	12,000
32	90	23	67	6	540
33	80	19	70	130	10,400
34	80	17	63	80	53,400
35	80	22	81	2	160
36	80	20	74	230	23,000
38	80	20	74	235	23,400
39	80	26	96	0.5	40

†Estimated error ± 5%

*Estimated error in counting total number of cycles

± 25% below 1,000 cycles

± 15% between 1,000 cycles and 10,000 cycles

± 5% above 10,000 cycles

All specimens failed.

TABLE 5

Static Tests of Group (2) Specimens (Scale Reinforced Concrete Beams)

Beam No.	P, Failing Load, lbs.*
97	620
67	580
50	560
11	600
40	545
88	525
68	660
100	575
	585 lbs. (Average)

* ● 10 lbs. Estimated error

Moment at static failing load, $M_{max} = \frac{P}{4}(L - a)$

$= \frac{585}{4}(23.5 - 4)$

$= 2850$ in. - lb.

$G_{ult} = \frac{4 f^2 L^2}{E I g} M_{max}$, pinned-pinned beam.

$= \frac{4 \times f^2 \times 23.5^2}{2.5 \times 10^6 \times 0.426 \times 386} \times 2850$

$= 1.53 \times 10^{-2} \times f^2$ g, peak .

Ultimate stress, $\sigma_{ult} = \frac{M_{max}\, c}{I}$

$= \frac{2850 \times 0.83}{0.426} = 5650$ psi (Bending) .

TABLE 6

Dynamic Tests of Group (2) Specimens, with
Sinusoidal Input to the Shaker

Excitation Frequency was 5% to 10% Higher than the Specimen Resonance Frequency

Beam	%Load†	Total Cycles*	Remarks
4	45	5.3×10^6	Broke at 3" from center
5	51	1.95×10^6	Broke at 1.5" from center
6	60	1.51×10^6	Severely cracked at center
7	77	9.45×10^4	Severely crackedat center
8	85	2.94×10^4	Broke at 1" from center
9	81	2.32×10^4	Broke at 1/2" from center
10	73	9.30×10^3	Severely cracked
12	77	5.5×10^4	Broke
13	81	7.23×10^4	Severely cracked, frequency down to 35~
14	73	9.8×10^3	Severely cracked
15	68	1.15×10^5	Severely cracked at center, 35~
16	77	6.5×10^4	Broke
17	73	1.38×10^5	Broke
18	68	4.37×10^5	Severely cracked, frequency 35~
19	64	2.64×10^5	Severely cracked, frequency 40~
20	68	2.44×10^5	Severely cracked, frequency 40~
21	73	1.029×10^5	Severely cracked at center
22	77	1.41×10^5	Cracked 4" from center, frequency 30~
23	81	1.168×10^5	Cracked at center, frequency 30~
24	68	8.01×10^5	Cracked at center, frequency 30~
25	64	1.98×10^5	Cracked 4.5" off center, frequency 25~
26	85	1.95×10^4	Broke
27	73	3.43×10^5	Broke
28	60	2.18×10^5	Broke 8.0" from center, Cracked at center
29	64	2.25×10^5	Severely cracked at center

TABLE 6 (Continued)

Beam	%Load†	Total Cycles*	Remarks
30	89	1.51×10^5	Severely cracked at center
31	81	2.54×10^5	Severely cracked at center
32	64	7.69×10^5	Severely cracked at center, frequency 30~
33	60	4.95×10^5	Frequency 38~
34	85	2.16×10^4	Severely cracked at center
35	81	8.55×10^4	Severely cracked at center
36	64	2.90×10^5	Broke 1" from center
37	60	3.68×10^5	Severely cracked 1/2" from center
38	55	3.86×10^5	Severely cracked at center
39	51	4.12×10^5	Severely cracked 1/2" from center
40	55	3.29×10^5	Broke 1" from center
41	116	8.25×10^3	Broke 1/2" from center
42	99	1.09×10^4	Broke 2" from center
49	99	8.14×10^3	Severely cracked at center
54	64	9.71×10^4	Severely cracked at center
55	64	4.54×10^5	Severely cracked at center
56	58	4.49×10^5	Broke 2" from center
57	58	3.24×10^5	Broke 1/2" from center
58	52	6.57×10^5	Broke 1" from center
59	52	3.64×10^5	Broke in center
60	52	1.86×10^5	Broke 1/2" from center

†Estimated error ± 5%

*Estimated error in counting total number of cycles

± 25% below 10,000 cycles
± 15% between 10,000 and 100,000 cycles
± 10% between 100,000 and 1,000,000 cycles
± 5% above 1,000,000 cycles

TABLE 7

Dynamic Tests of Group (2) Specimen, with Random Input (20-220 Cycles, Flat) to the Shaker ‡

Beam No.	Input† g rms	$\frac{g_{peak}}{G_{ult}}$	Approx. No. of Cycles *	Comments
65	2	0.17	1,070,000	Broke
66	3	0.26	2,396,000	Did not fail
69	6	0.50	45,000	Broke
70	4.5	0.39	427,000	Broke
71	2.5	0.25	6,157,000	Did not fail
72	2.5	0.21	1,197,000	Broke
73	10	0.85	15,000	Broke
74	10	0.85	5,000	Broke
75	8	0.68	12,000	Broke
76	8	0.68	22,000	Broke
77	6	0.50	21,000	Broke
78	6	0.50	42,000	Broke
79	4	0.34	532,000	Broke
80	4	0.34	367,000	Broke
81	10	0.85	7,000	Broke
82	8	0.68	24,000	Broke
83	6	0.50	44,000	Broke
84	4	0.34	300,000	Broke
85	2	0.17	1,471,000	Did not fail
86	2	0.17	1,646,000	Did not fail
87	12	1.02	4,000	Broke

† Estimated error ± 20%

‡ Estimated error ± 10%

*Estimated error in counting total number of cycles:

± 50% below 10,000 cycles
± 25% between 10,000 and 100,000 cycles
± 10% between 100,000 and 1,000,000 cycles
± 5% above 1,000,000 cycles

TABLE 8

Test Data Sheet Evaluated from a Typical Test Record
Beam No. 84 Under Random Vibration

4 g rms Input ; $S_{\ddot{W}_o}(\omega_1) = 0.08\ g^2/cps.$

Time	Δ Time Minutes	$S_{\ddot{W}_1}(\omega_1)^*$ g^2/cps	$R = \frac{S_{\ddot{W}_1}(\omega_1)}{S_{\ddot{W}_o}(\omega_1)}$	$Q = \sqrt{\frac{R}{1.6}}$	f* cps	Total Cycles
1840	Start				100	6,000
1841	1	5.2	65	6.4	86	16,300
1843	2	6.3	79	7.0	82	36,000
1847	4	7.5	94	7.7	80	40,800
1851	4	6.0	75	6.8	80	45,600
1855	4	5.0	62.5	6.2	76	54,600
1905	10	5.0	62.5	6.2	74	98,600
1910	5	5.2	65	6.4	76	121,400
1920	10	4.8	60	6.1	74	165,600
1925	5	5.5	69	6.5	76	188,400
1940	15	4.0	50	5.6	72	253,400
1950	10	4.0	50	5.6	72	297,400
1953	1	2.0	25	3.5	60	300,400
1953	End	Beam Broke				

*Estimated Average Value during Time Interval.

8.0 CONCLUSIONS

The following conclusions are derived from the observation of the experimental tests. They are listed arbitrarily with no sequence of importance.

(1) The stress-cycle, S-N, curves of the reinforced concrete for the dynamic tests differ quite markedly from that of the zero-to-maximum repeated loading. The differences are:

(i) Apparently no endurance limit can be determined up to 10^6 cycles.

(ii) The dynamic ultimate strength, from the sinusoidal dynamic test, is at least 20% higher than the static ultimate strength. (See Figure 21) A figure of 30 to 40 percent higher, as suggested by some investigators,* is reasonable.

(iii) The S-N curves of the dynamic tests are shifted to the right with a much steeper negative slope than that of the slow, repeated zero-to-maximum loading test.

(2) The concrete beams in both groups (1) and (2) were found to be not quite uniform in their physical properties. This was particularly true of the beams in group (1) which were signified by the non-uniform static failing loads in the static test. Initial cracks could be found in some of these beams. Some test data, therefore, was discarded when the beams tested were believed to be abnormal.

(3) The use of strain gages for strain measurement of the beams under dynamic tests was not successful due to surface cracks.

(4) It was observed, particularly from the random test records, that the dynamic magnification factor, Q, of the reinforced concrete beams, changed continuously as the total number of vibration cycles increased. In some cases, the value of Q dropped from the initial value of 8 or 9 to 2 or 3 at the end of a test before the beam failed. Special tests for the Q measurement were performed by low level discrete frequency scans at intervals during a few fatigue tests. Typical results of these tests are presented in Figures 17 and 18. The lowering of the Q values signified the increase of the internal damping of the test specimen. The variation of Q in the random tests was summarized in Figures 24 through 26.

---

* See No. 21 in Bibliography for example.

(5) The resonant frequency of the beam specimens lowered continuously as the load cycles increased. This lowering could be due to :

(i) Readjustment of end fixity at the beginning of a test run.

(ii) The gradual increase of damping.

(iii) Micro and/or macro cracks result in change of bending stiffeners, E I, of the test specimen.

(6) The control of the stress level, experienced by the specimen under dynamic test, by means of the relative acceleration method, proved to be reliable and made this experiment feasible. By this method, the test specimen could actually be vibrated at the resonant frequency in the sinusoidal test experiment. However, because of the frequency sensitivity at resonance, the continuous decrease of resonant frequency, change in damping of the beam, and the non-linear vibration behavior of the specimen, off-resonant frequency excitation was employed. A vibration frequency of 10 to 15 percent below the specimen's fundamental frequency was used for the weaker group (1) specimen, and 5 to 10 percent higher frequency values were employed for the stronger group (2) specimen. The relative acceleration was noted to be much increased in the higher-than-resonant frequency test as the middle of the beam and the supports were vibrated out-of-phase. This off-resonance test should be noted to have no significant effect on the stress calculation. Figure B1 of Appendix B shows that the mode shape is essentially a half-sine wave, as in the case of resonance, even when the ratio of excitation frequency to the resonance frequency, ω/ω_1, is as low as 0.5, or as high as 2.0.

(7) The accuracy in counting the vibration cycles of the test specimens became very difficult in the very short test runs with very high loads. These difficulties are illustrated by Figure 11 where a test beam failed before a very high load of constant acceleration could be maintained. The cycles accuracy becomes much improved for lower load and long duration tests as shown in Figures 9, 10, and 12.

(8) The stress-cycle (S-N) curves of the sinusoidal tests of the specimens in groups (1) and (2) are truly the commonly defined S-N curves, since the stress of each beam specimen was able to be maintained to a desired level throughout the entire duration of a test run, in spite of any change of the circumstance that might arrive from concrete cracking. However, it should be emphasized here that the stress-cycle curve of the random test is not truly a S-N curve in the sense that the stress changed continuously due to the rapid decrease of the dynamic magnification factor, Q, as test went on. In this latter case, the fatigue factor is defined only when the specimen is intact, uncracked, and experienced no severe vibration before.

9.0 COMMENTS

Despite many difficulties encountered in this experimental study of the dynamic fatigue properties of reinforced concrete, the test method appeared to be feasible and yielded meaningful data. The test specimens, specially manufactured for this experiment, were carefully scaled versions of a full size beam structure. The dynamic fatigue properties of the scaled specimens could therefore, be used for further structural design. The size factor was not investigated. However, using the knowledge gained from the steel fatigue problems, the author feels that a size factor of one could be safely used in evaluating larger concrete structures from this model beam study. Since the smaller size specimens are generally weaker due to the fact that they are more easily influenced by local stress concentration, the application of the test data taken from the smaller model beams to the larger structure is on the conservative side.

The accuracy in estimating the total cycles of vibration at high dynamic loads, in both sinusoidal and random input tests, was quite low. The test specimens might break very rapidly, a matter of a few seconds to a few minutes. It also took time to bring the acceleration up to a desired level, and time to record data. However, this accuracy improved significantly for the long duration and low dynamic load tests.

The desired acceleration level was controlled manually and was subject to human error and limitation. No automatic feedback control was employed, so that the shaker would not be greatly overloaded and damaged at the moment the test beam failed.

The strength of the concrete varies significantly from one sample to another, from one batch of mix to another, from one source of material supply to another, and for many other reasons. The experimental data of this report could be influenced by the material selection and special attention in fabrication. Similar tests should be performed for a better understanding of concrete under dynamic loads, on larger scale structure, with various qualities of aggregates and cement, various mix ratio, various water content, and with and without additive. Nevertheless, the results obtained in this experiment provide a useful comparison of random and sinusoidal fatigue of concrete and extensive data on fatigue due to repeated single-direction loads.

Appendix C presents four examples to illustrate the fatigue life estimation of concrete beams using data charts compiled from this experimental study. These examples are intended for beams subjected to random vibration with their end conditions either pinned or clamped. The usefulness of these data charts can be further extended to the plate problems, such as concrete structural walls, by using the plate theories which are available in many standard text books.

BIBLIOGRAPHY

1. Bate, S.C.C., "The strength of Concrete Members under Dynamic Loading", A symposium on the strength of concrete structure, Cement and Concrete Association, London, 1956.

2. Penzion, J. and Hansen, R.J., "Static and Dynamic Elastic Behavior of Reinforced Concrete Beams", J. of Am. Concrete Inst., Vol. 25, No. 7, March 1954, pp. 545-567.

3. Nordby, G.M., "Fatigue of Concrete - A Review of Research", J. of Am. Concrete Inst., Vol. 30, No. 2, August 1958, pp. 191-220.

4. Williams, H.A., "Fatigue Test of Light Weight Aggregate Concrete Beams", J. of Am. Concrete Inst., Vol. 14, No. 5, April 1943, pp. 441-447.

5. Chang, T.S. and Kesler, C.E., "Fatigue Behavior of Reinforced Concrete Beams", J. of Am. Concrete Inst., Vol. 30, No. 2, August 1958, pp. 245-254.

6. Mudrock, J.N. and Kesler, C.E., "Effect of Range of Stress on Fatigue Strength of Plain Concrete Beans", J. of Am. Concrete Inst., Vol. 30, No. 2, August 1958, pp. 222-231.

7. Stelson, T.E. and Cernica, J.N., "Fatigue Properties of Concrete Beams", J. of Am. Concrete Inst., Vol. 30, No. 2, August 1958, pp. 255-260.

8. Etkin, Y., "A Study of the Resonant Frequencies of Prestressed Concrete Floor Beams", Thesis presented to the University of London for the degree of M. Sc. (Eng.) 1956.

9. Chang, T.S. and Kesler, C.E., "Static and Fatigue Strength in Shear of Beams with Tensile Reinforcement", J. of Am. Concrete Inst., Vol. 29, No. 12, No. 12, June 1958, pp. 1033-1057.

10. Mavis, F.T. and Stewart, "Further Tests of Dynamically Loaded Beams", J. of Am. Concrete Inst., Vol. 30, No. 11, May 1959, pp. 1215-1223.

11. Vallette, R., "Endurance of Reinforced Concrete Railway Bridges Tests of Beams with Repeated Bending", Intern. Assoc. for Bridge and Structural Eng., Vol. 8, 1947.

12. ACI Committee 215, "Fatigue of Concrete", ACI Bibliography No. 3, Am. Concrete Inst., Detroit, Mich., pp, 38, 1960.

13. Verna, J.R. and Stelson, T.E., "Failure of Small Reinforced Concrete Beam under Repeated Loads", ACI J., Proceedings, Vol. 59, No. 10, October 1962, pp. 1489-1504.

14. Oladapo, J.O., "Rate of Loading Effect on Moment-Curvature Relation in Prestressed Concrete Beams", J. of Am. Concrete Inst., p. 871.

15. Verna, J.R., "The Effect of Sustained and Repeated Loads on Reinforced Concrete Beams", a PhD Thesis, Carnegie Inst. of Technology, Pittsburgh, Pa. 1960.

16. "Austrian Fatigue Tests of Reinforced Concrete Beams", Engineering News-Record, May 16, 1935 and October 31, 1935, p. 697.

17. Allgood, J.R., Bate, S.C.C., Mavis, F.T., McKee, K.E., "Comparison of Prestressed Concrete Beams and Conventional Reinforced Concrete Beams under Impulsive Loading", J. of Am. Concrete Inst., Part 2, June 1962, pp. 873-884.

18. Reinschmidt, K.F., Hansen, R.J. and Yang, C.Y., "Dynamic Tests of Reinforced Concrete Columns", J. of Am. Concrete Inst., March 1964, pp. 317-332.

19. Sinha, B.P., Gerstle, K.H. and Tulin, L.G., "Stress-Strain Relations for Concrete under Cyclic Loading," J. of Am. Concrete Inst., February 1964, pp. 195-205.

20. Verna, J.R. and Stelson, T.E., "Repeated Loading Effect on Ultimate Static Strength of Concrete Beams", J. of Am. Concrete Inst., June 1963, pp. 743-749.

21. Norris, Hansen, Holley, Biggs, Namyet, and Minami, Structural Design for Dynamic Loads, McGraw-Hill, 1959.

22. Goldsmith, W. Polivka, M. and Yang, T., "Dynamic Behavior of Concrete", J. of Soc. for Experimental Stress Analysis, Vol. 6, No. 2, February, 1966.

23. Snowden, J.C., "Transverse Vibration of Free-Free Beams", Journal Acoustic Society America, pp. 35-47, 1963.

24. McLachlan, N.W., Complex Variable and Operational Calculus, The Macmillan Company, New York, 1942.

25. Vigness, I., "Field Measurements and Testing", Random Vibration, Vol. II, Ch. 8, J. Wiley and Son, 1963.

26. Crandall, S.H. Editor, Random Vibration, Wiley and Son, 1958.

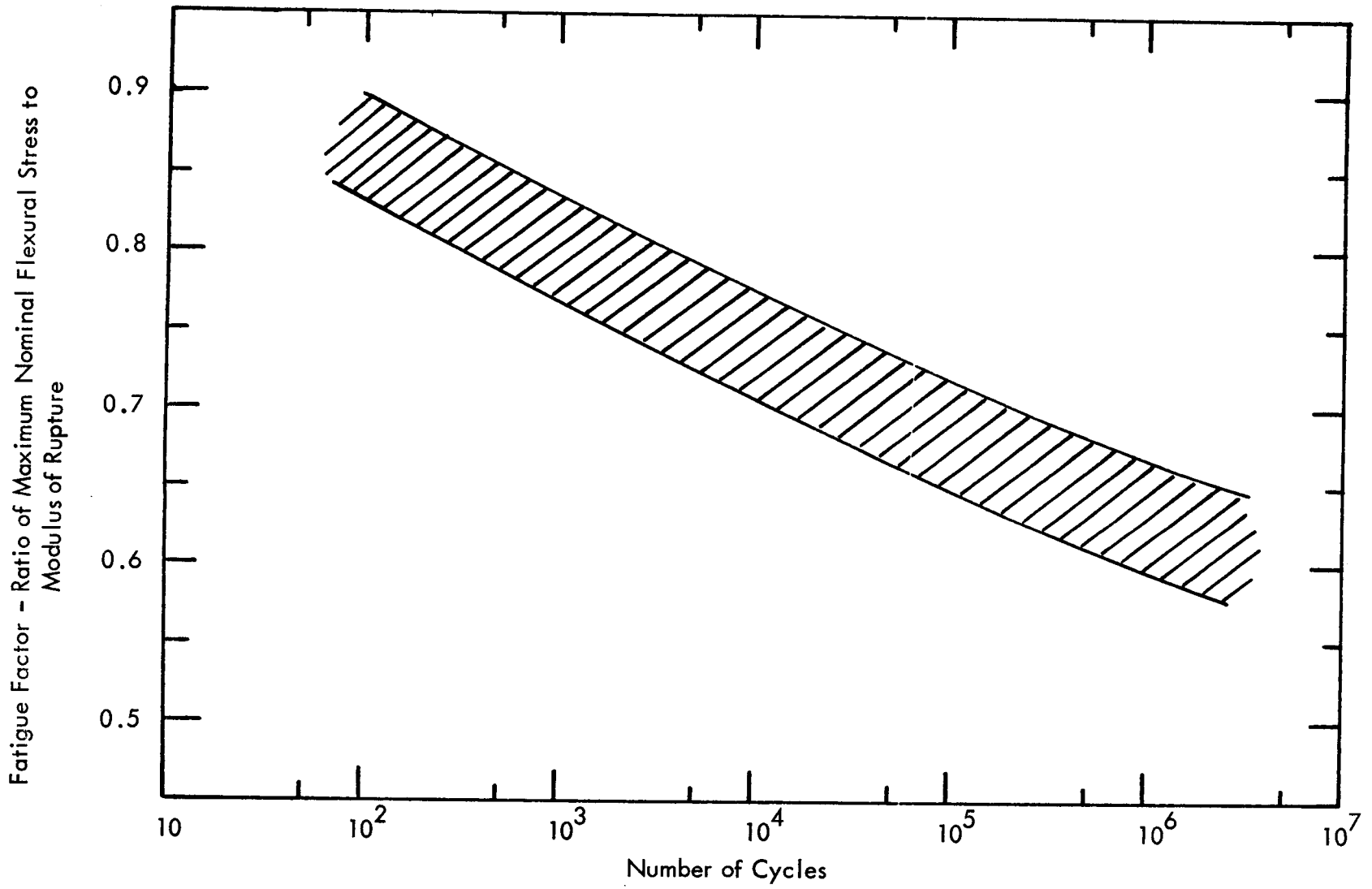

Figure 1. S-N Curve of Plain Concrete under Zero-to-Maximum Slow Repeated Loads.

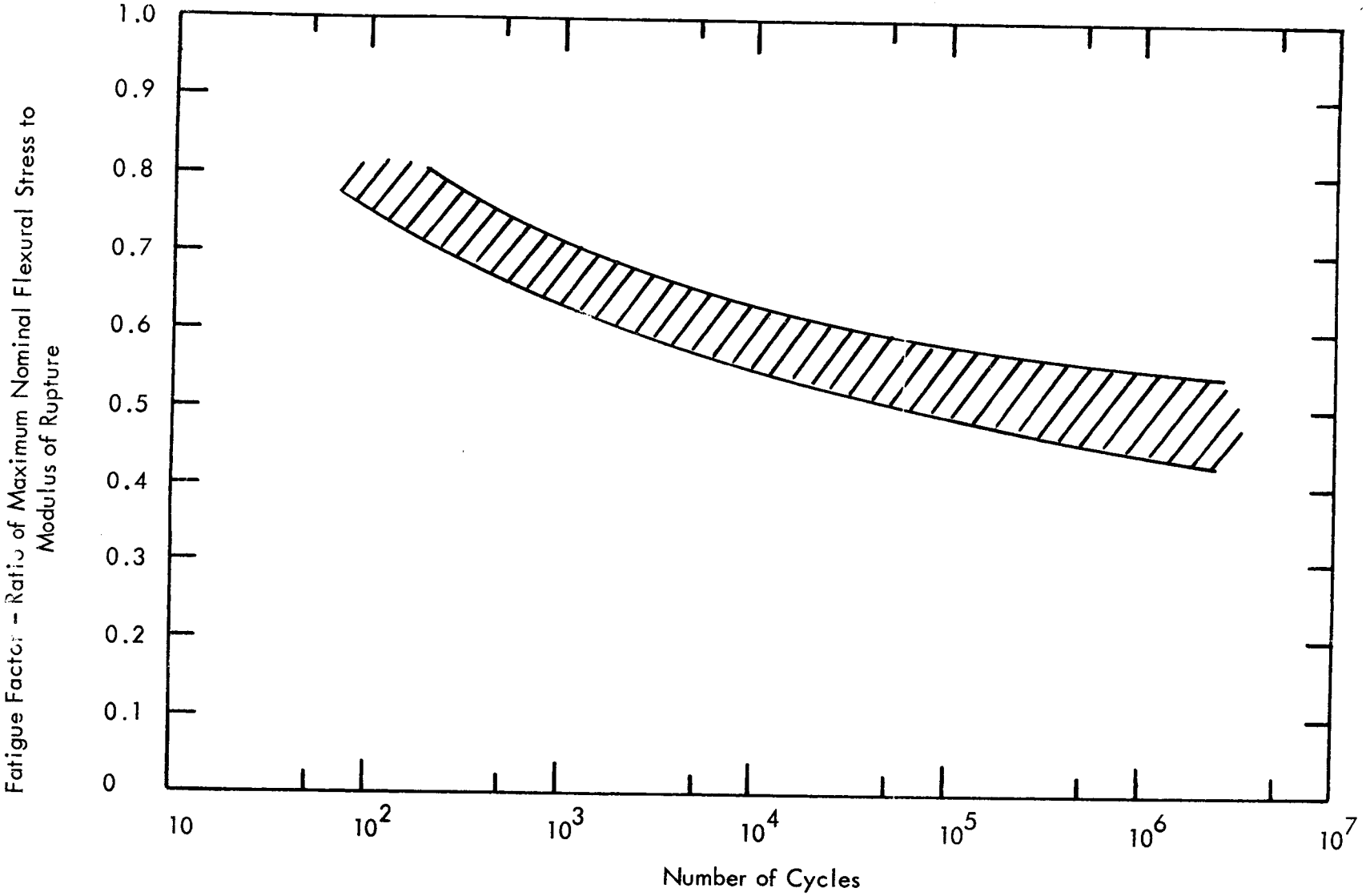

Figure 2. S-N Curve of Reinforced Concrete Subjected to Zero-to-Maximum Slow Repeated Loads.

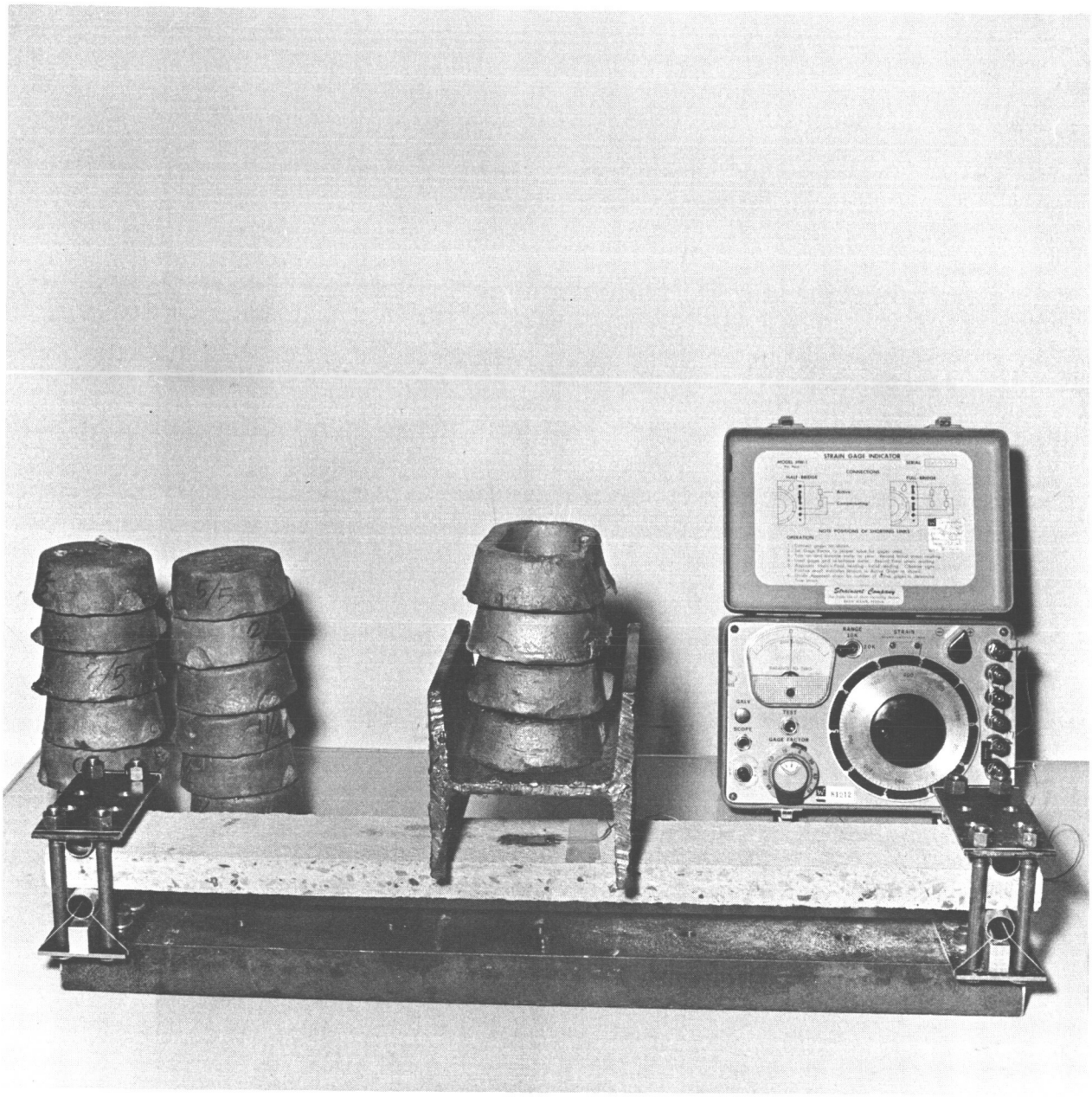

Figure 3. Simply Supported Concrete Beam under Static Test. Test Configuration 1.

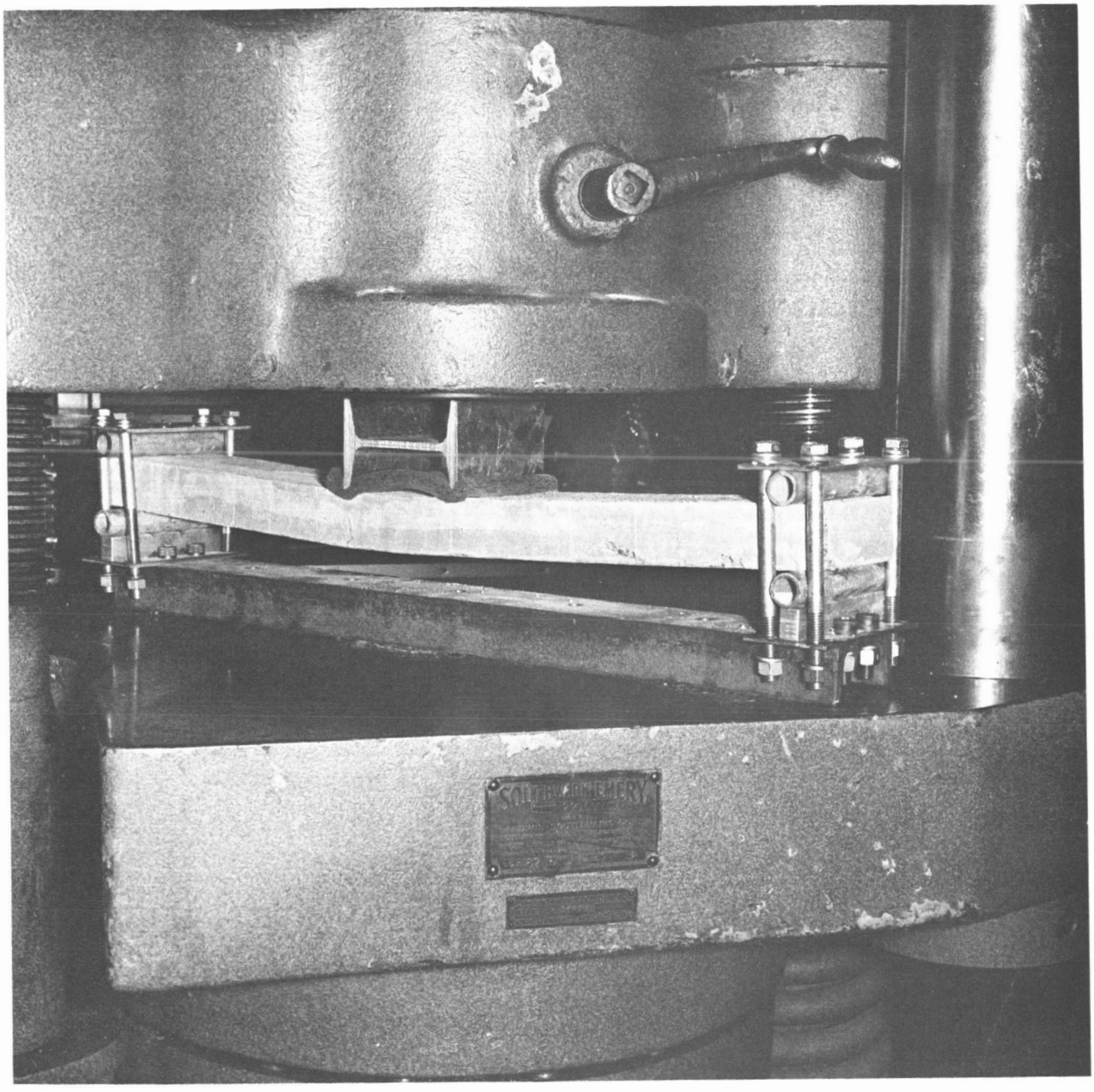

Figure 4: Simply Supported Concrete Beam Under Static Test.
Test Configuration 2.

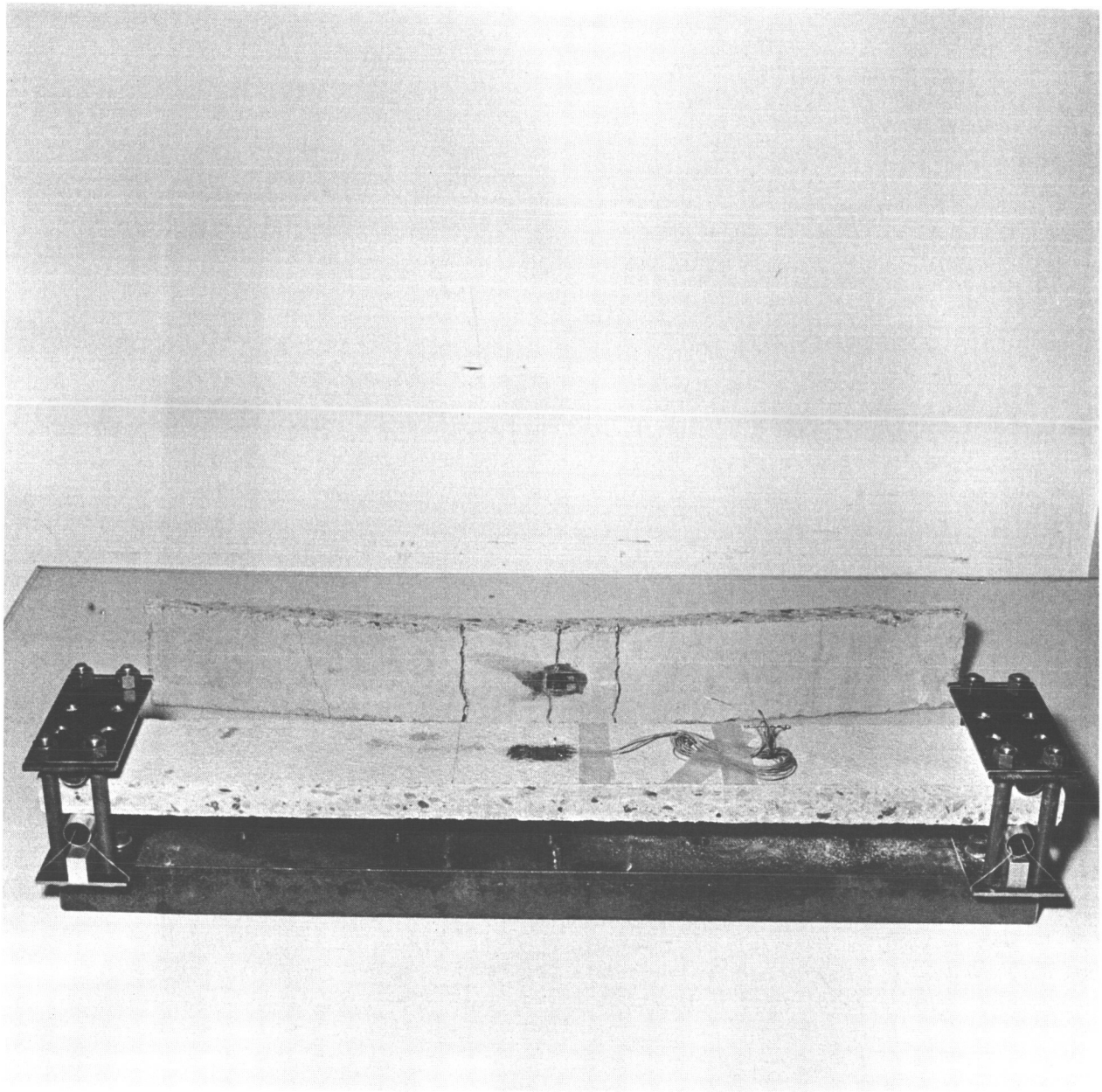

Figure 5. Concrete Beam Showing Supports in Detail and Typical Failure Mode of a Test Beam.

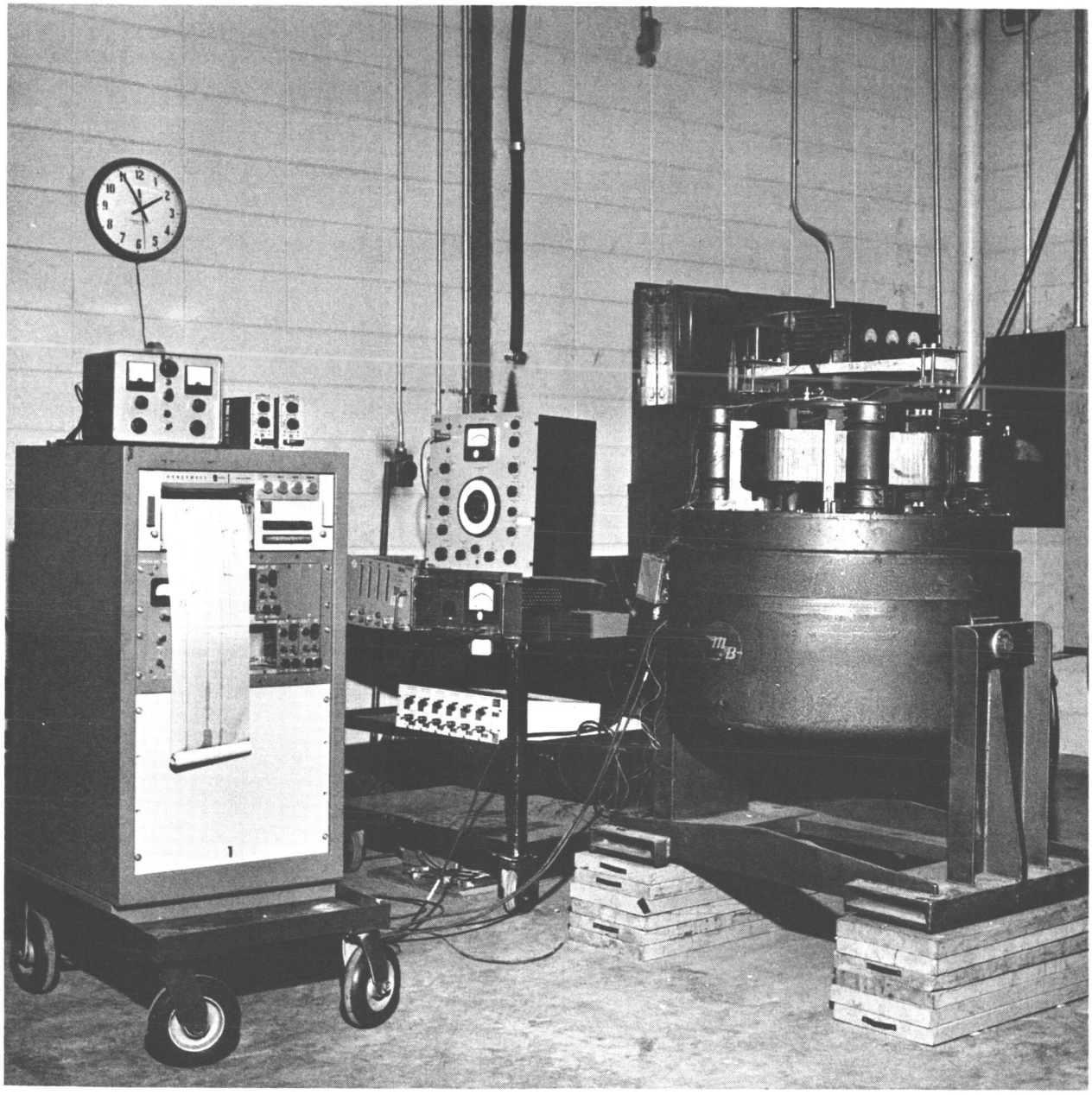

Figure 6. Equipment used in Dynamic Testing of a Concrete Beam.

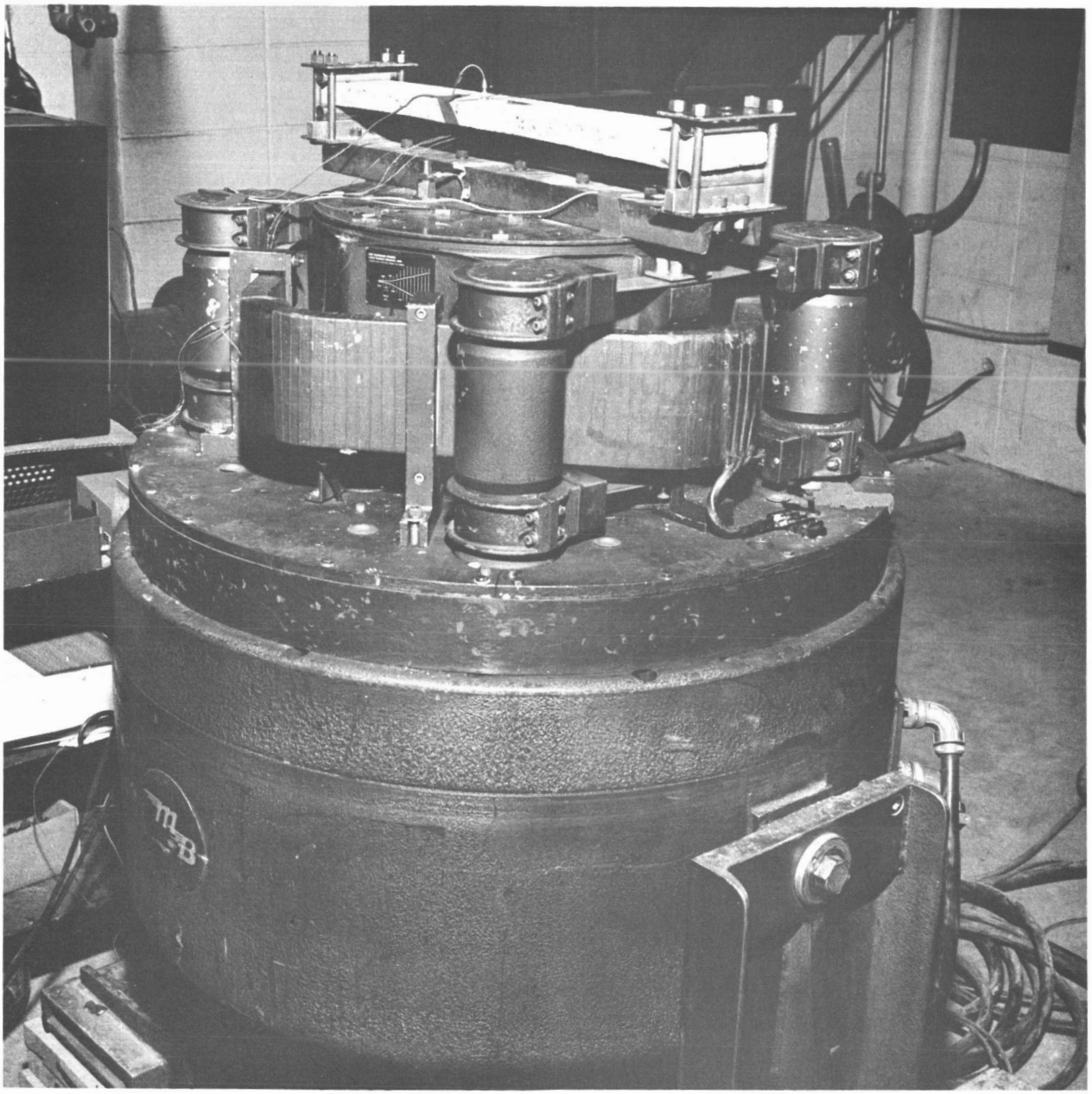

Figure 7: Dynamic Testing of a Concrete Beam Mounted on a MB C-25 HH Vibrator

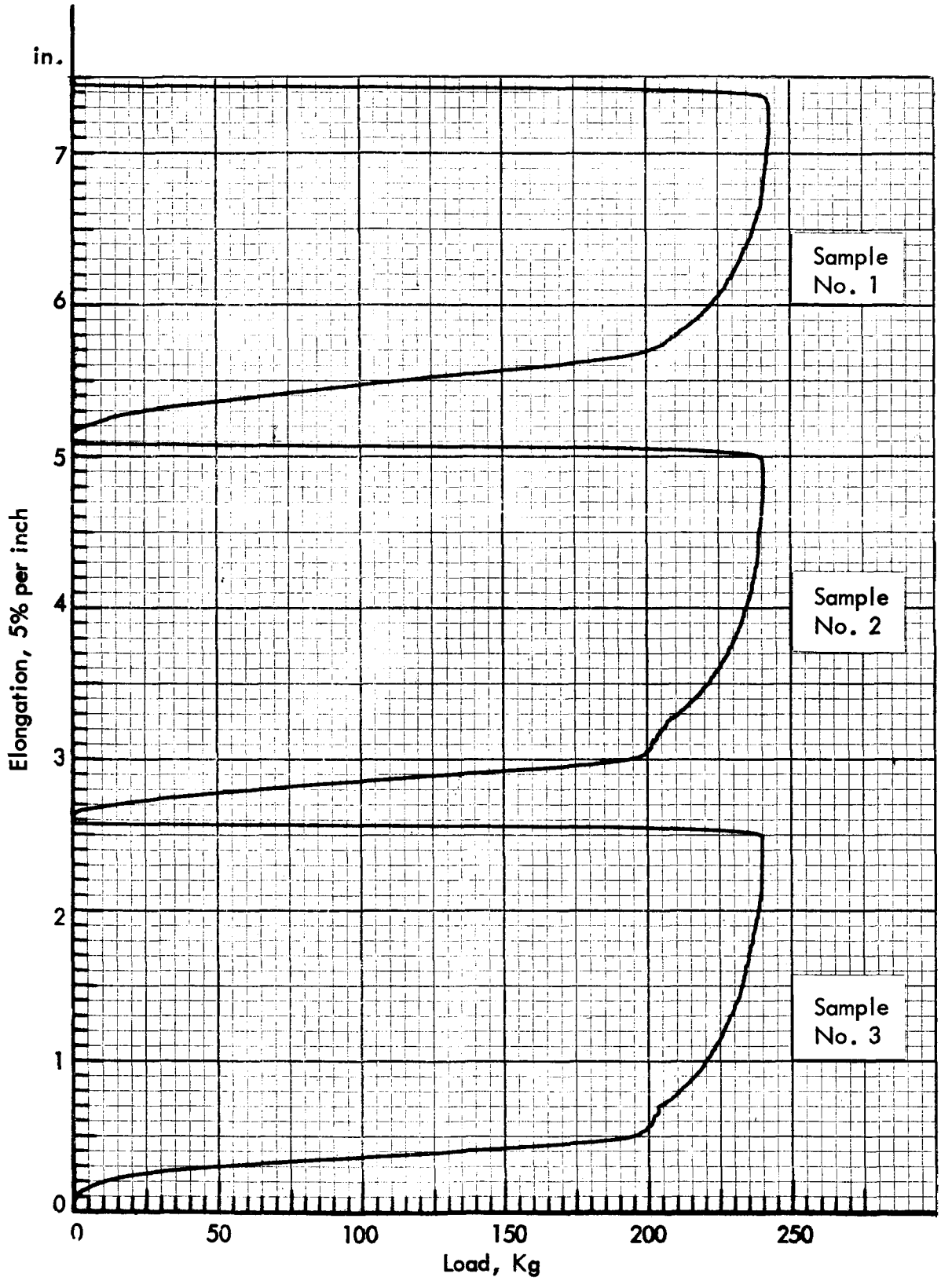

Figure 8 : Load-Elongation Curves of Commercial 12-1/2 Gage Wires (Diameter 0.10 inch)

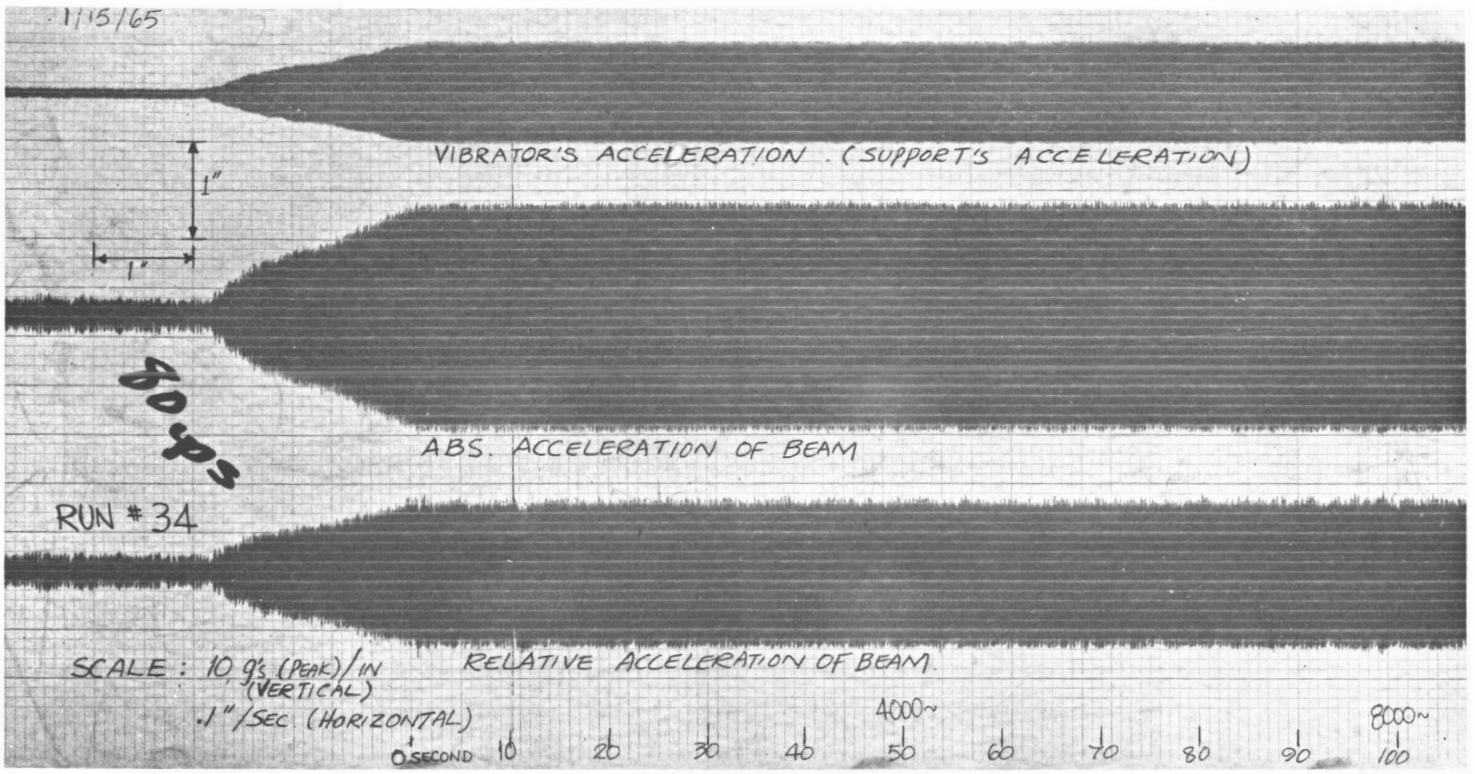

Figure 9. Run No. 34. Portion of a Typical Record of a Group (1) Specimen under Dynamic Sinusoidal Test.

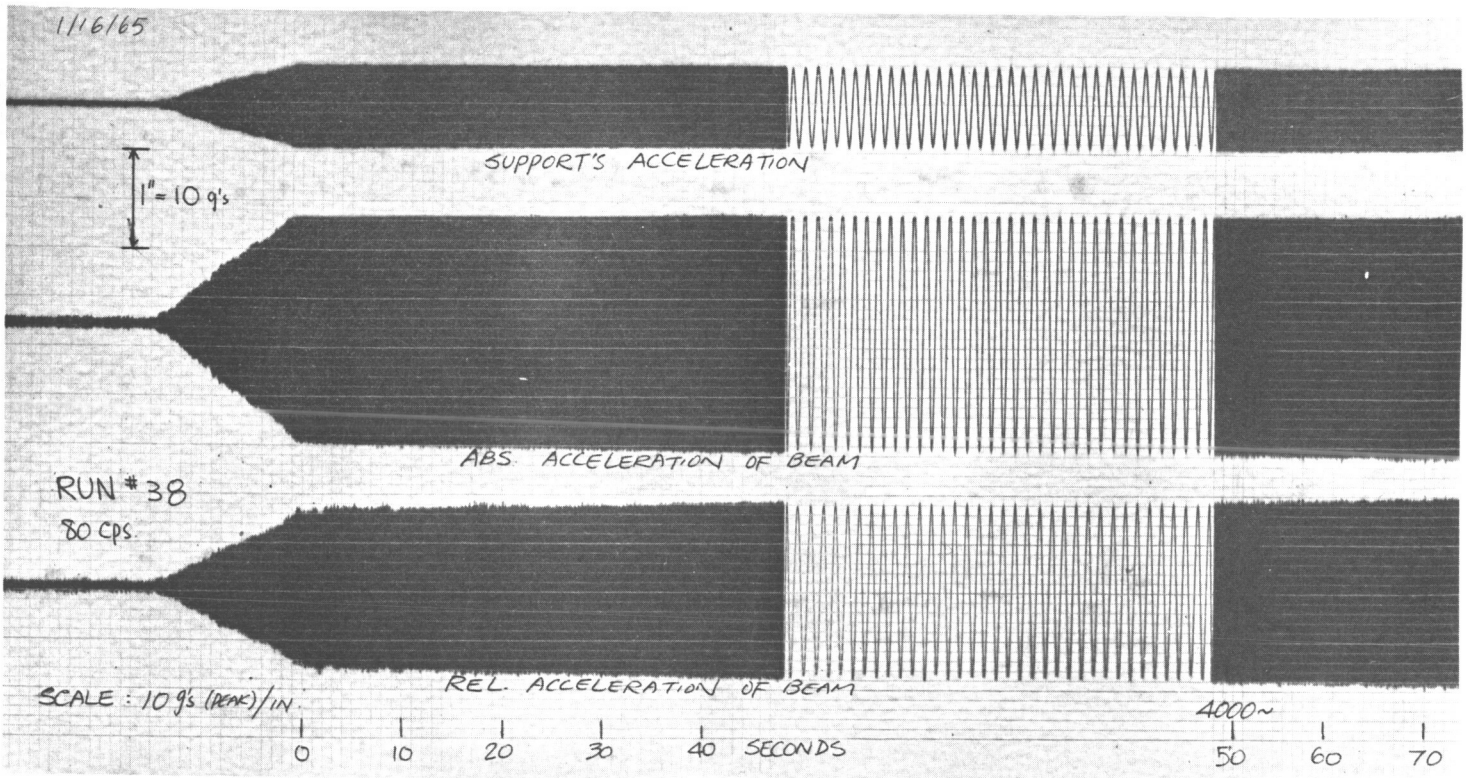

Figure 10. Run No. 38. Portion of a Typical Record of a Group (1) Specimen under Dynamic Sinusoidal Test.

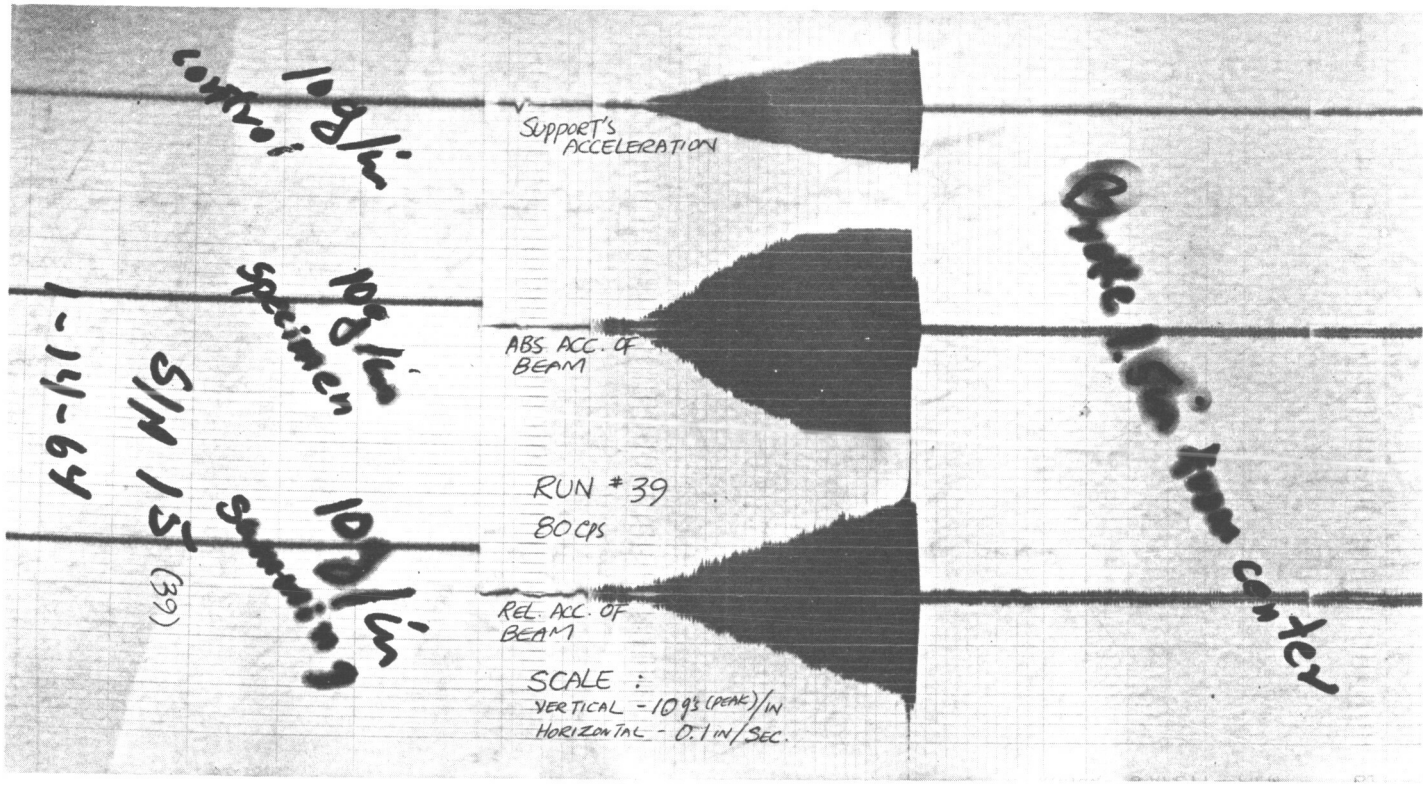

Figure 11. Run No. 39. A Typical Complete Record of a Group (1) Specimen under Dynamic Sinusoidal Test of very Short Duration.

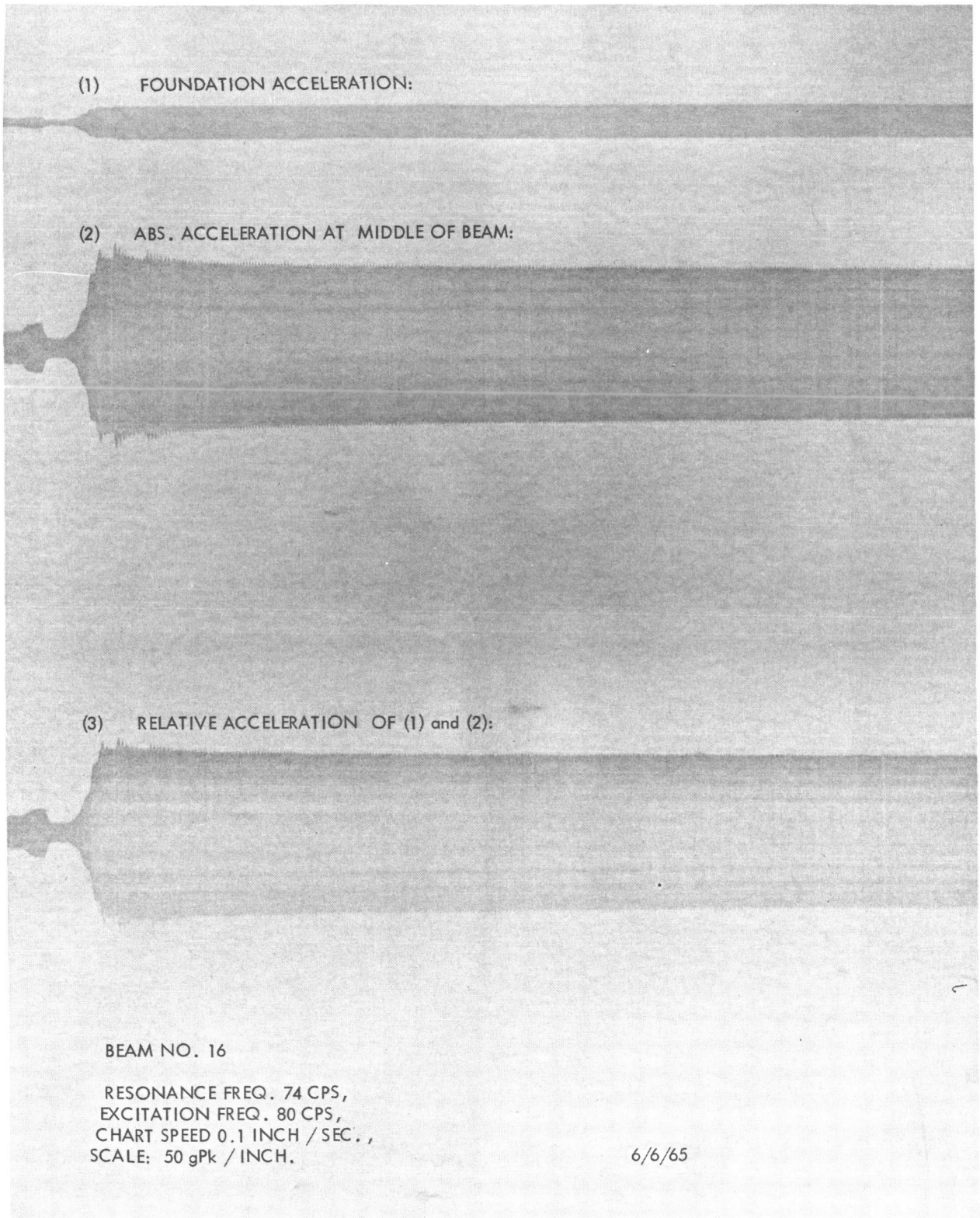

Figure 12. Beam No. 16. Portion of a Typical Record of a Group (2) Specimen under Dynamic Sinusoidal Test.

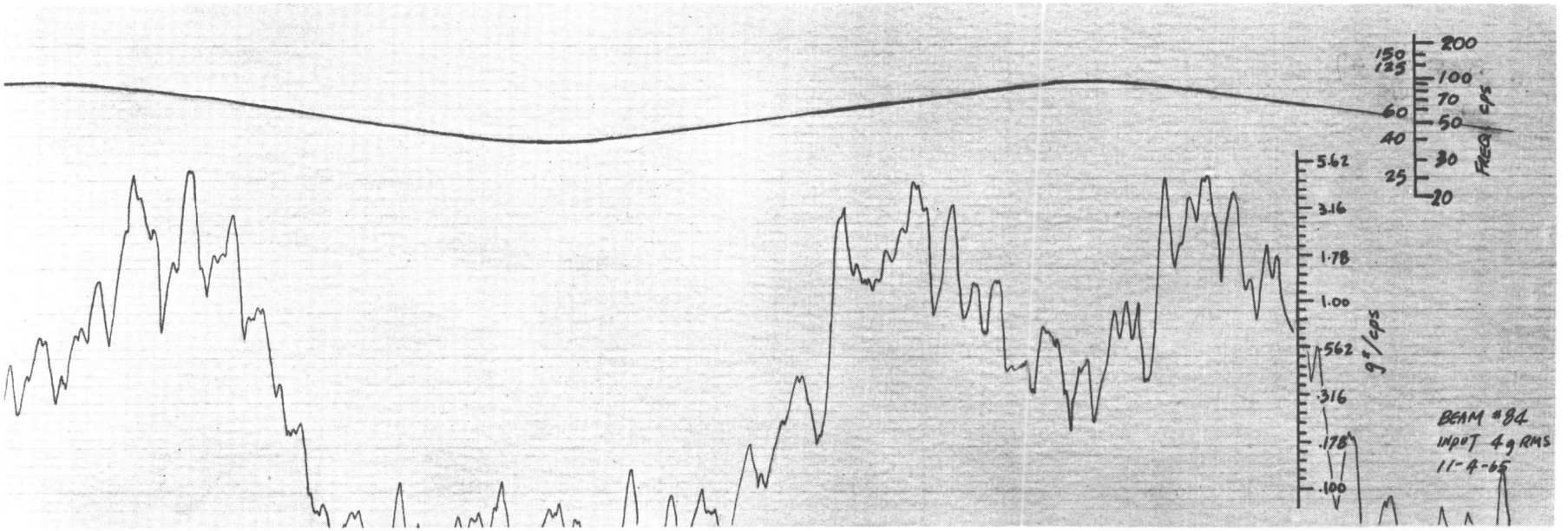

Figure 13. Beam No. 84. Portion of a Typical Record of a Group (2) Specimen under Dynamic Random Test; Fast Recording.

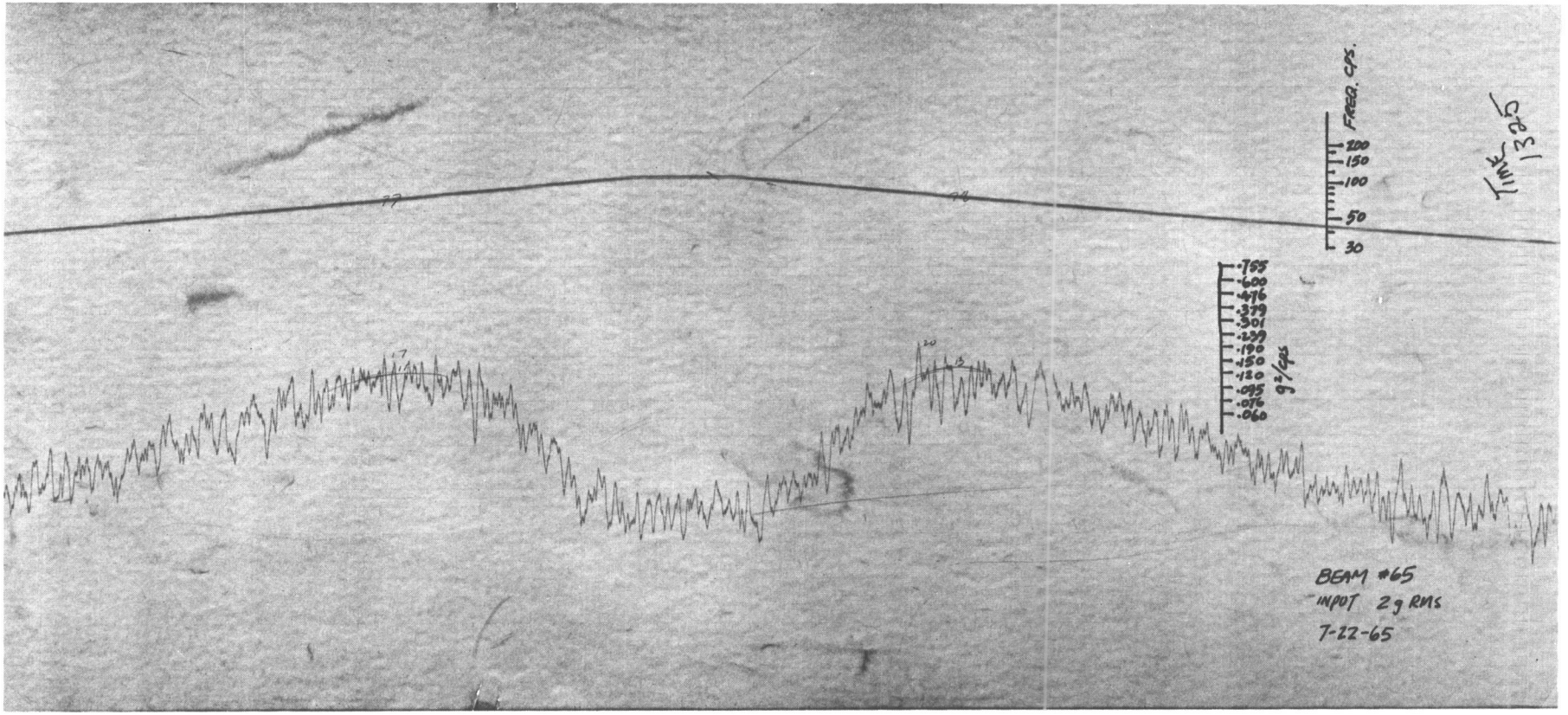

Figure 14. Beam No. 65. Portion of a Typical Record of a Group (2) Specimen under Dynamic Random Test; Fast Recording.

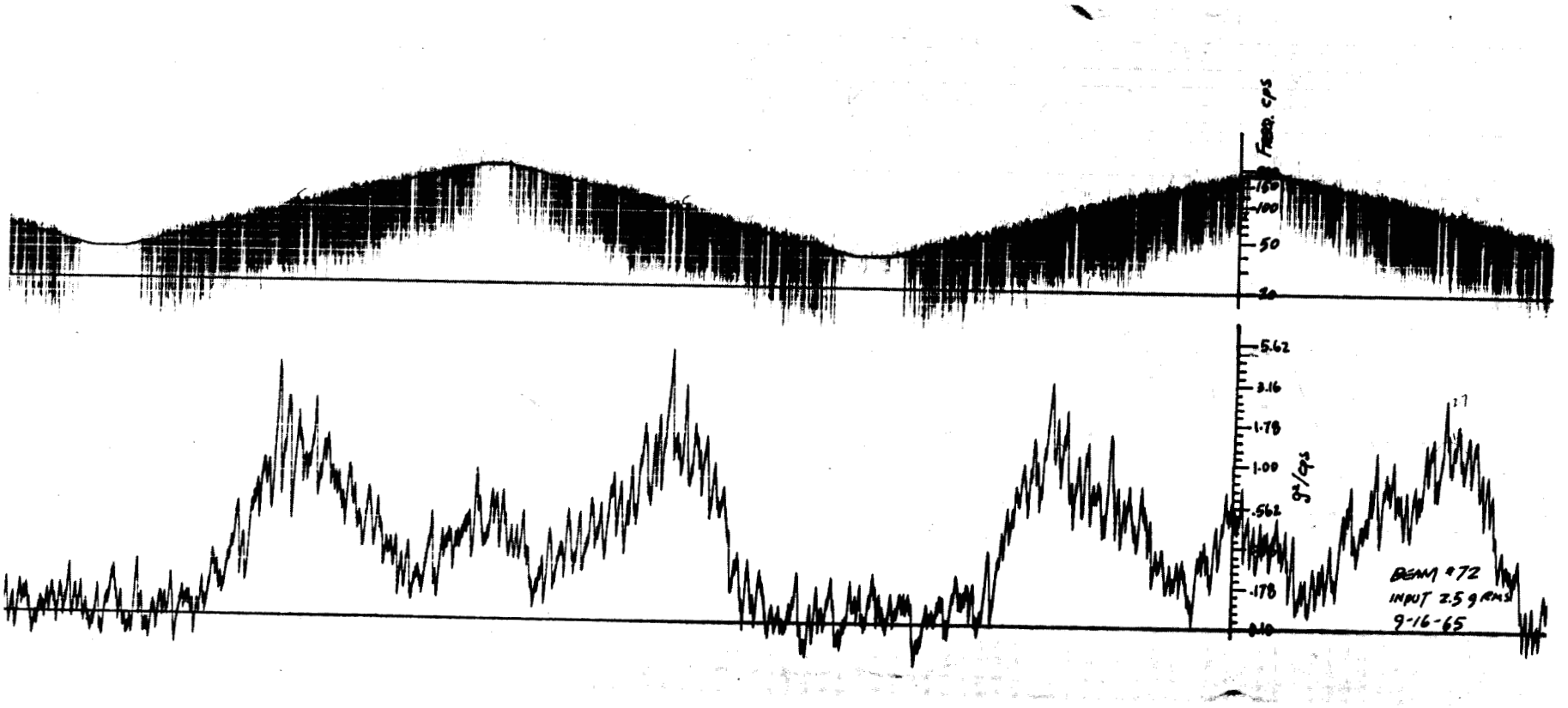

Figure 15. Beam No. 72. Portion of a Typical Record of a Group (2) Specimen under Dynamic Random Test; Slow Recording.

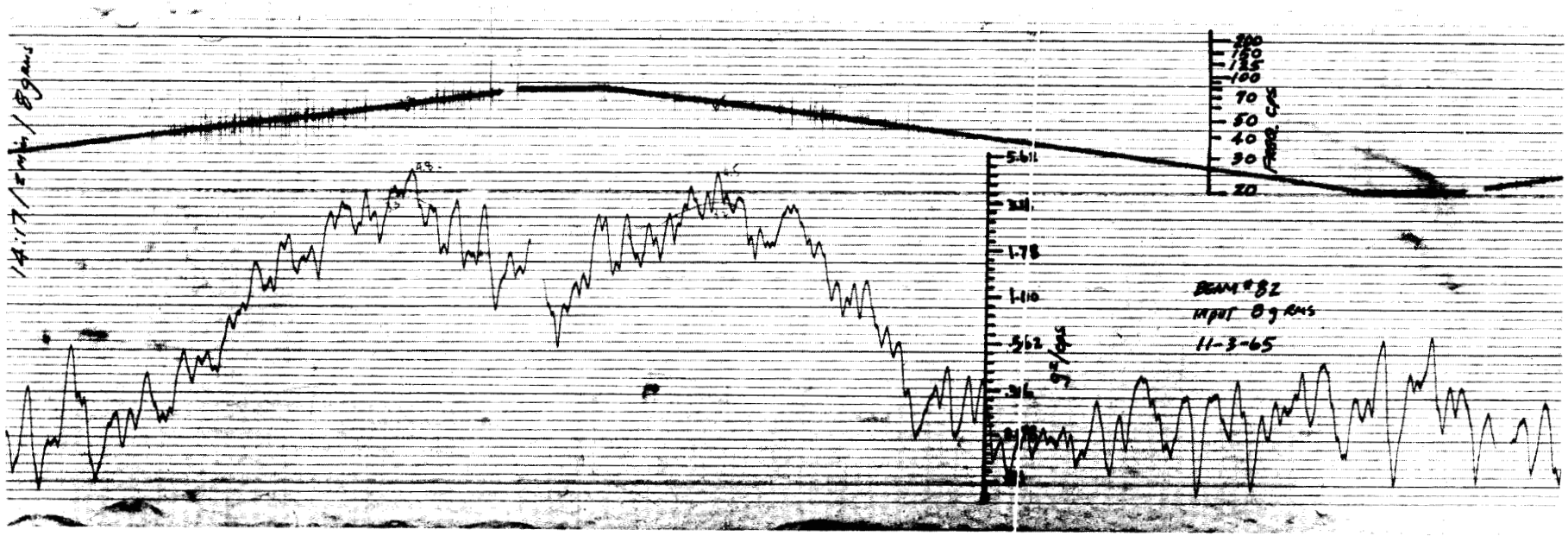

Figure 16. Beam No. 82. Portion of a Typical Record of a Group (2) Specimen under Dynamic Random Test.

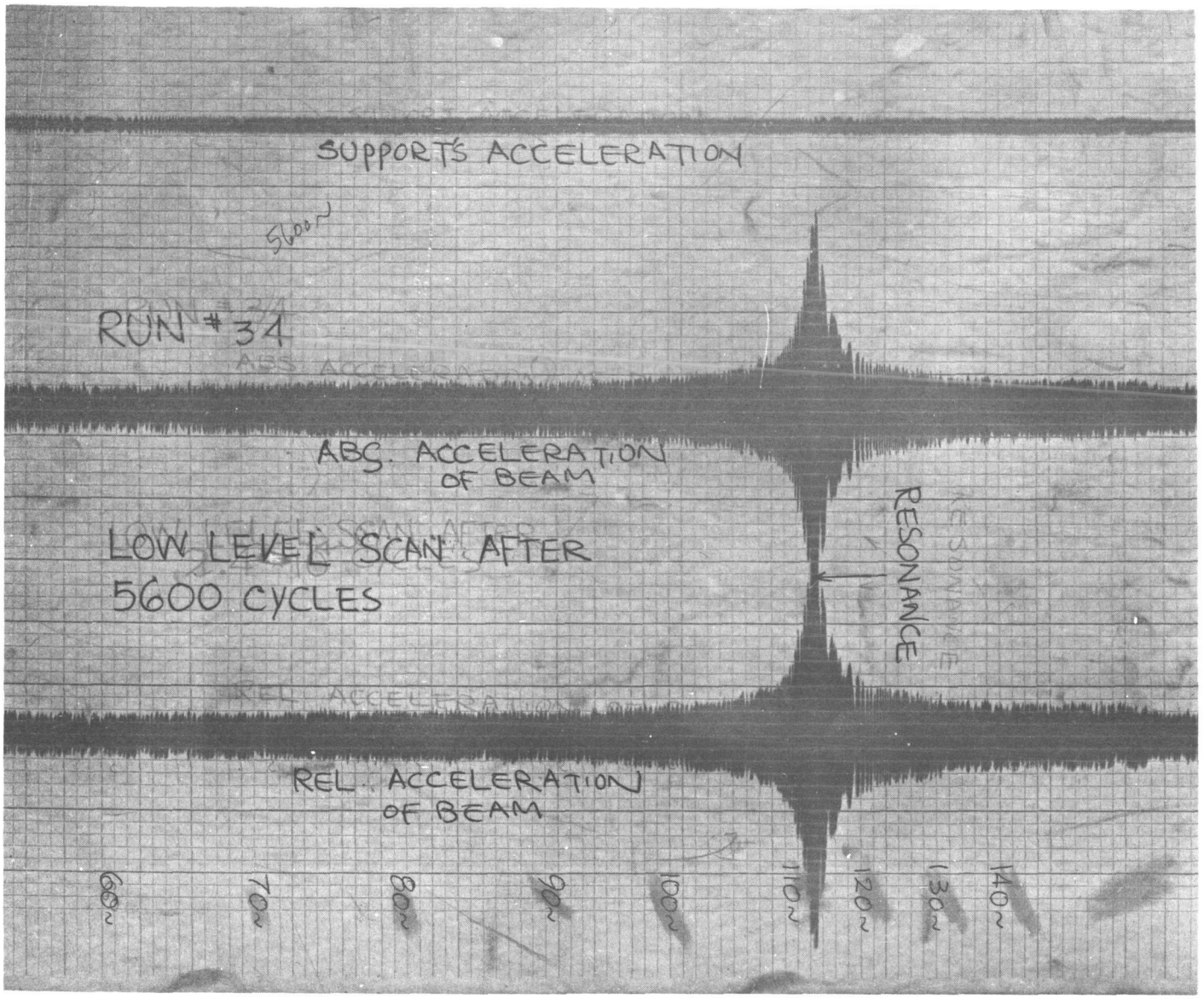

Figure 17. Low Level Scan of Run No. 34. After 5600 Cycles.

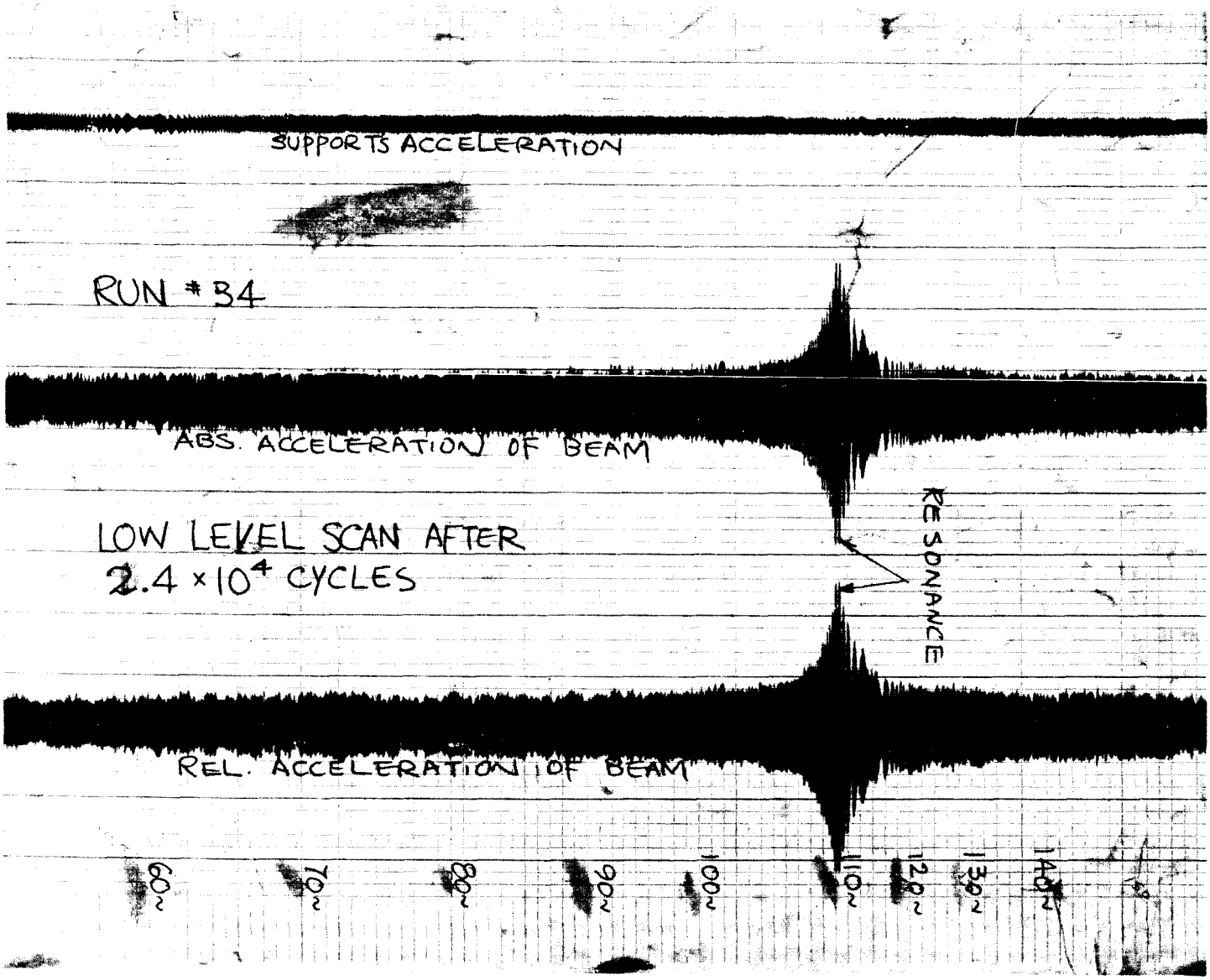

Figure 18. Low Level Scan Run No. 34 After 24,000 Cycles.

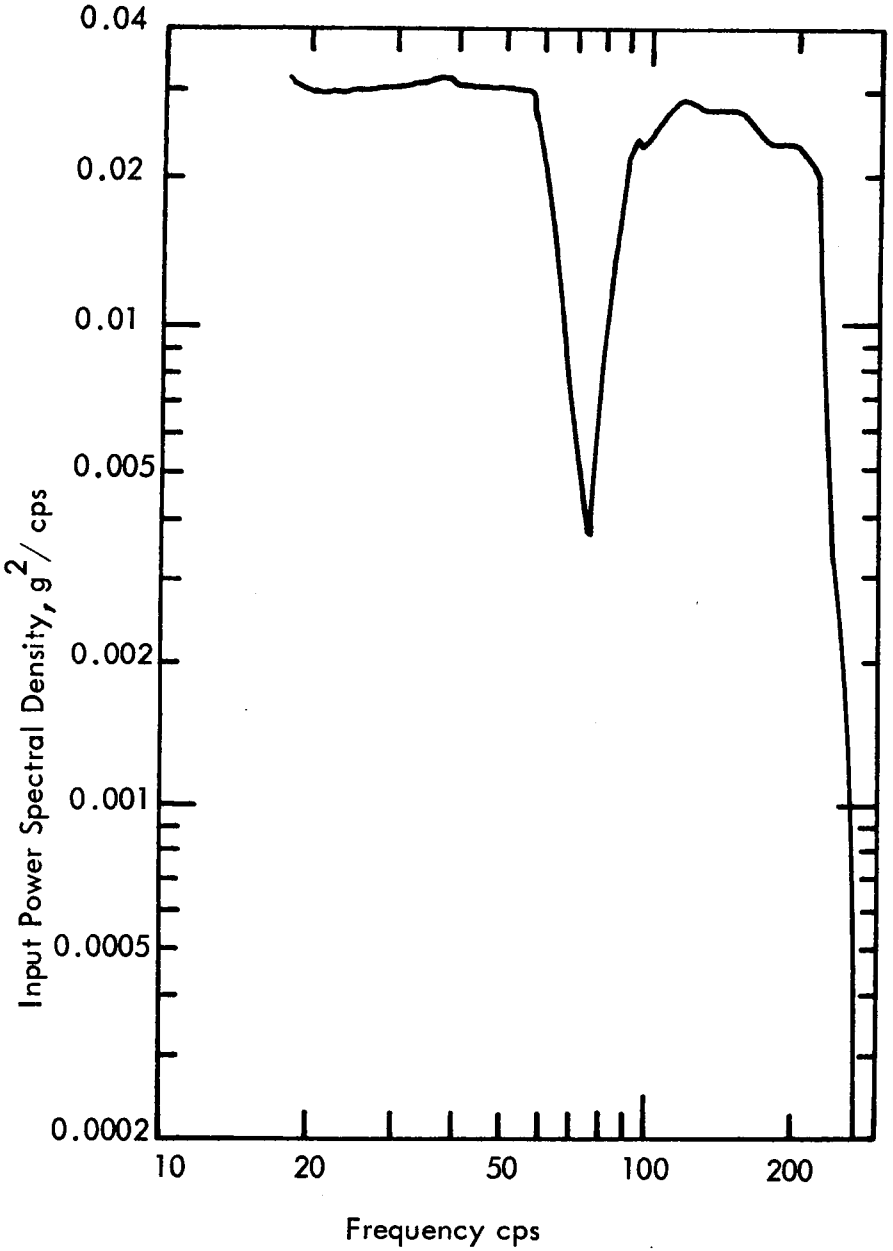

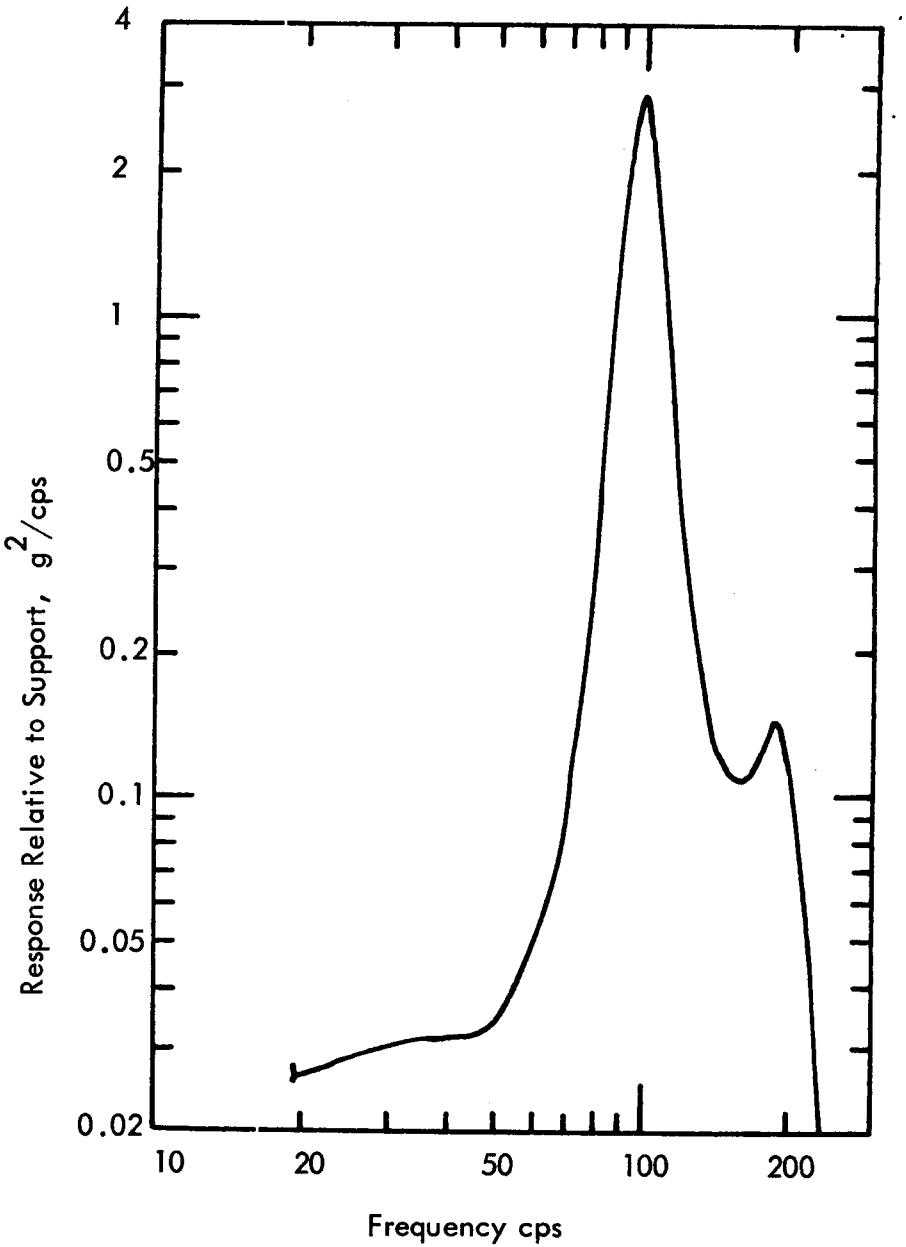

Figure 19. Typical Input and Response Power Spectral Densities of a Test Specimen under Random Vibration Test (Beam No. 84, 4 g rms Input to Shakers).

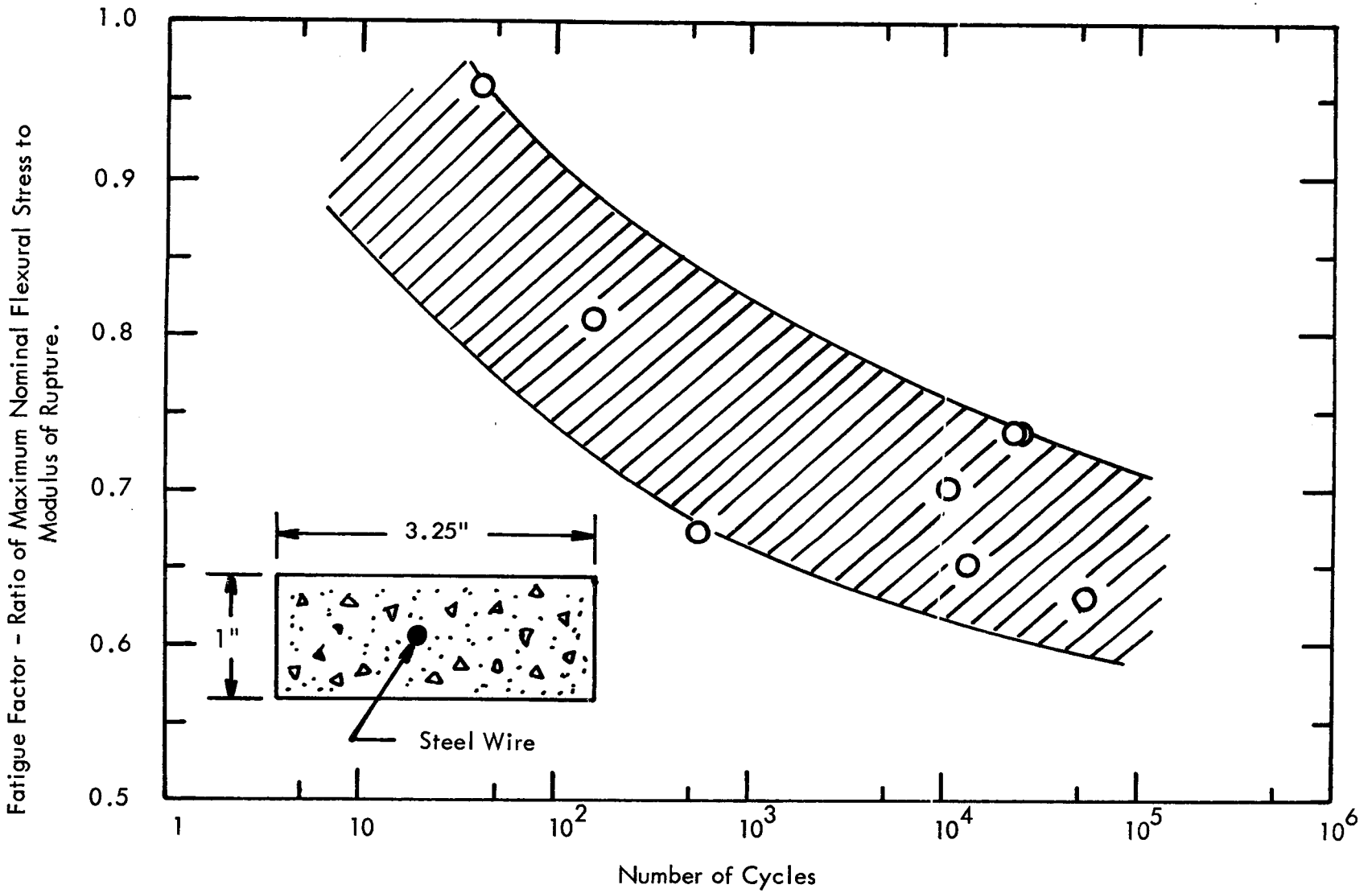

Figure 20. S-N Curve of Lightly Reinforced, Light Weight Concrete Beams, 1" x 3.25" x 23.5", under Dynamic Sinusoidal Loads.

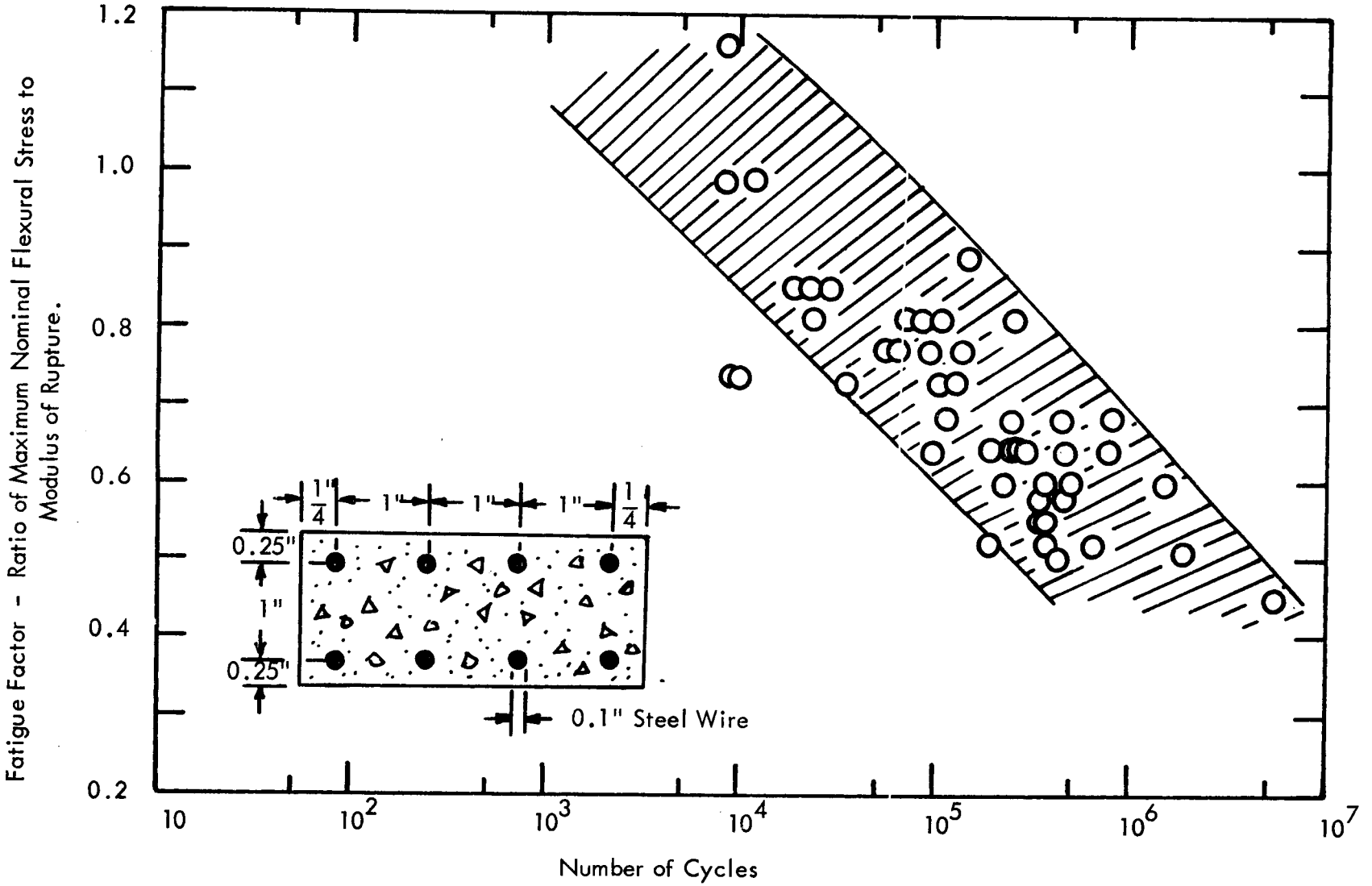

Figure 21. S-N Curve of Scale Reinforced Concrete Beam, 1.5" x 3.5" x 23.5", under Dynamic Sinusoidal Loads.

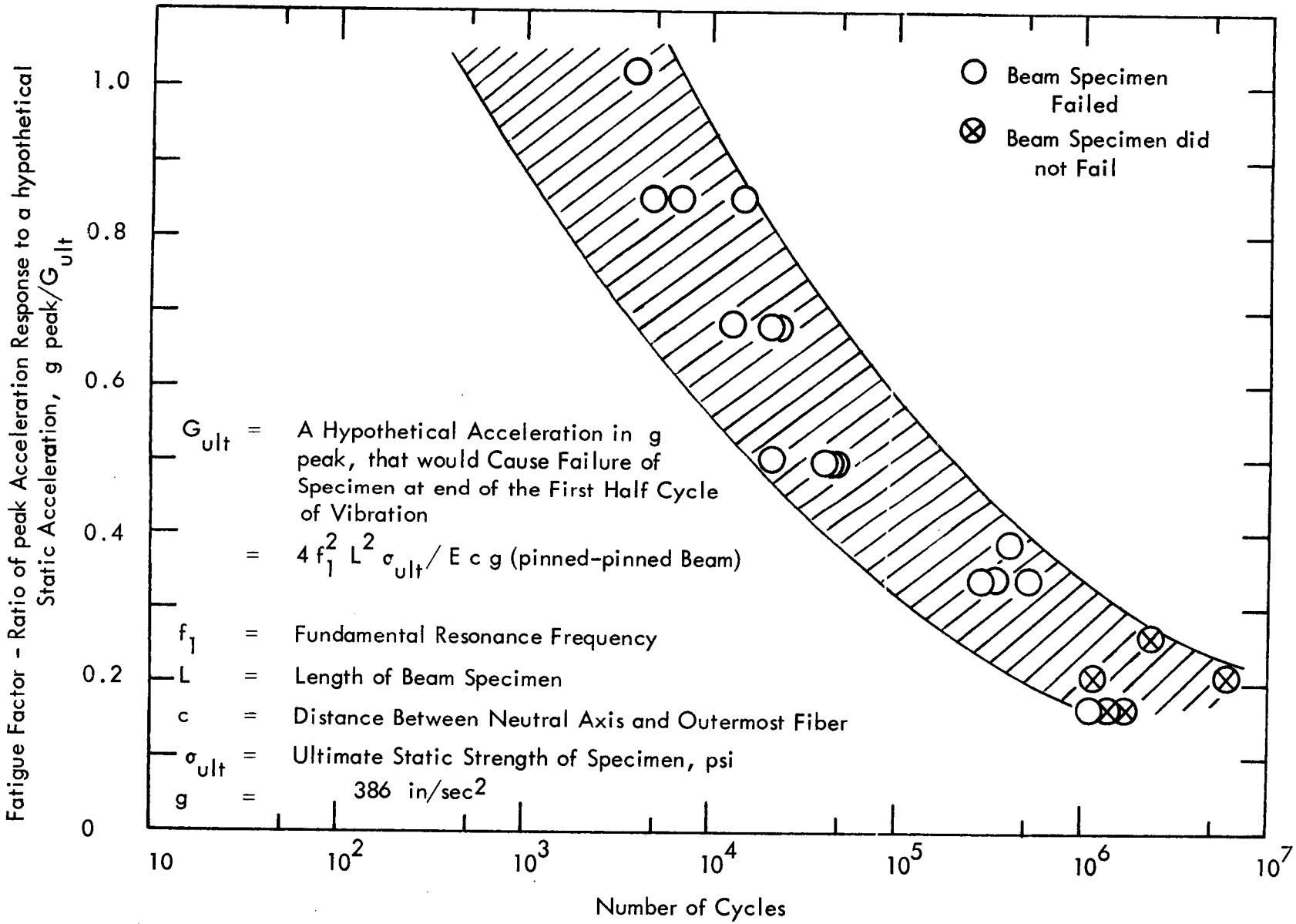

Figure 22. Fatigue Properties of Scale Reinforced Concrete Beams, 1.5" x 3.5" x 23.5", under Random Excitation. (Q = 8)

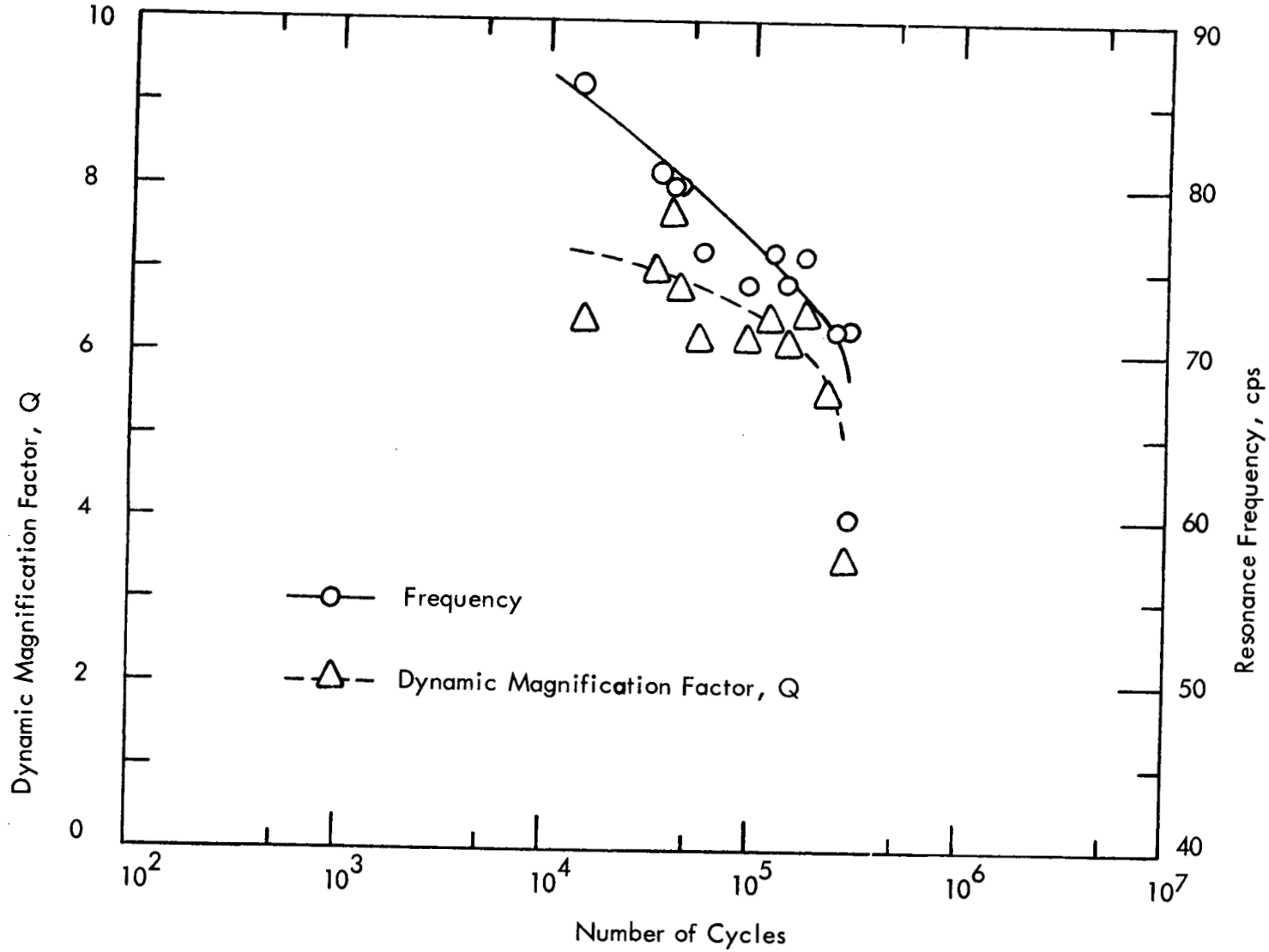

Figure 23. Drops of Resonance Frequency and the Dynamic Magnification Factor, Q, of a Typical Beam under Random Vibration in a Concrete Fatigue Test. (Beam No. 84)

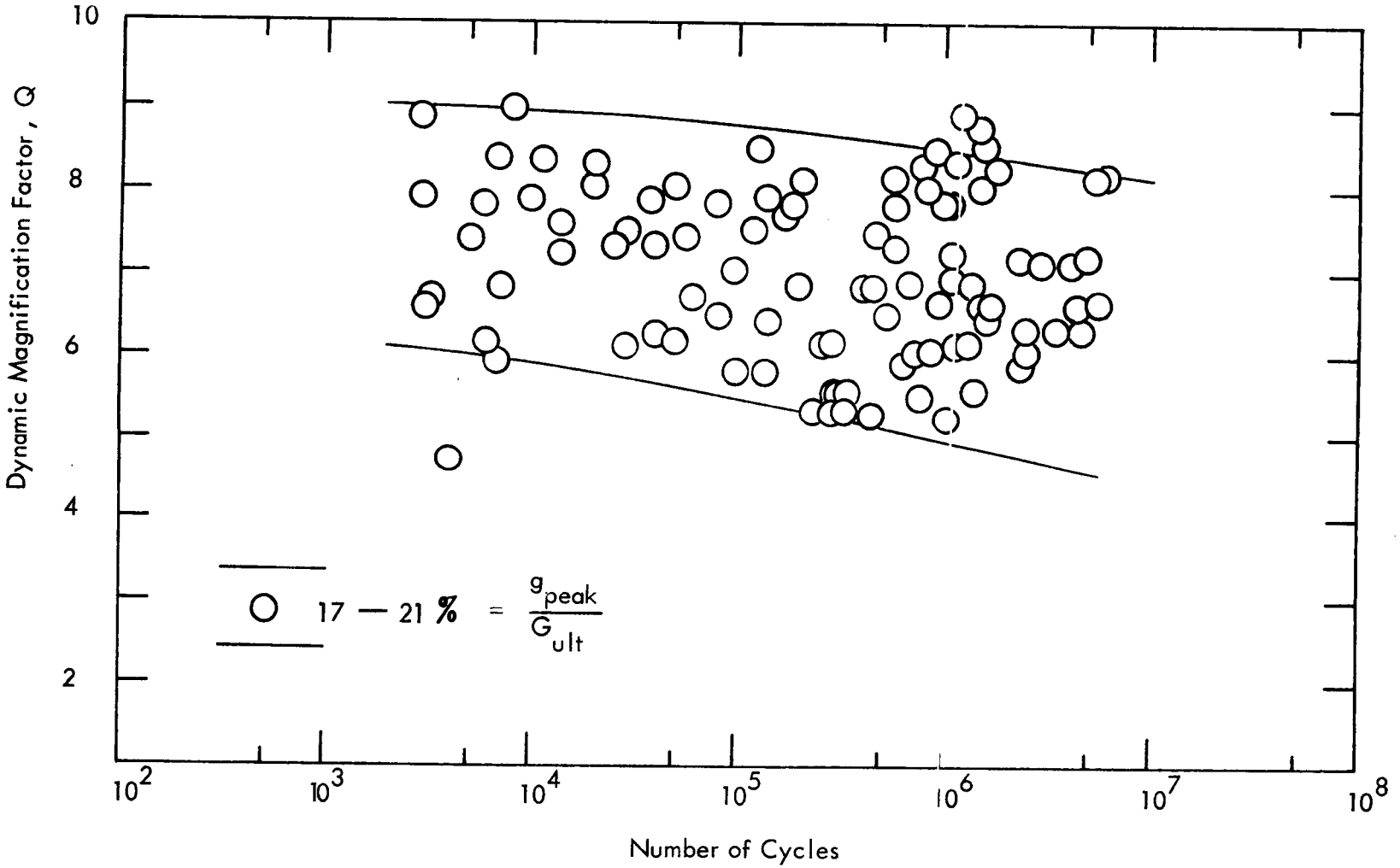

Figure 24. Variation of Dynamic Magnification Factor, Q, of Reinforced Concrete, Subjected to Random Vibration.

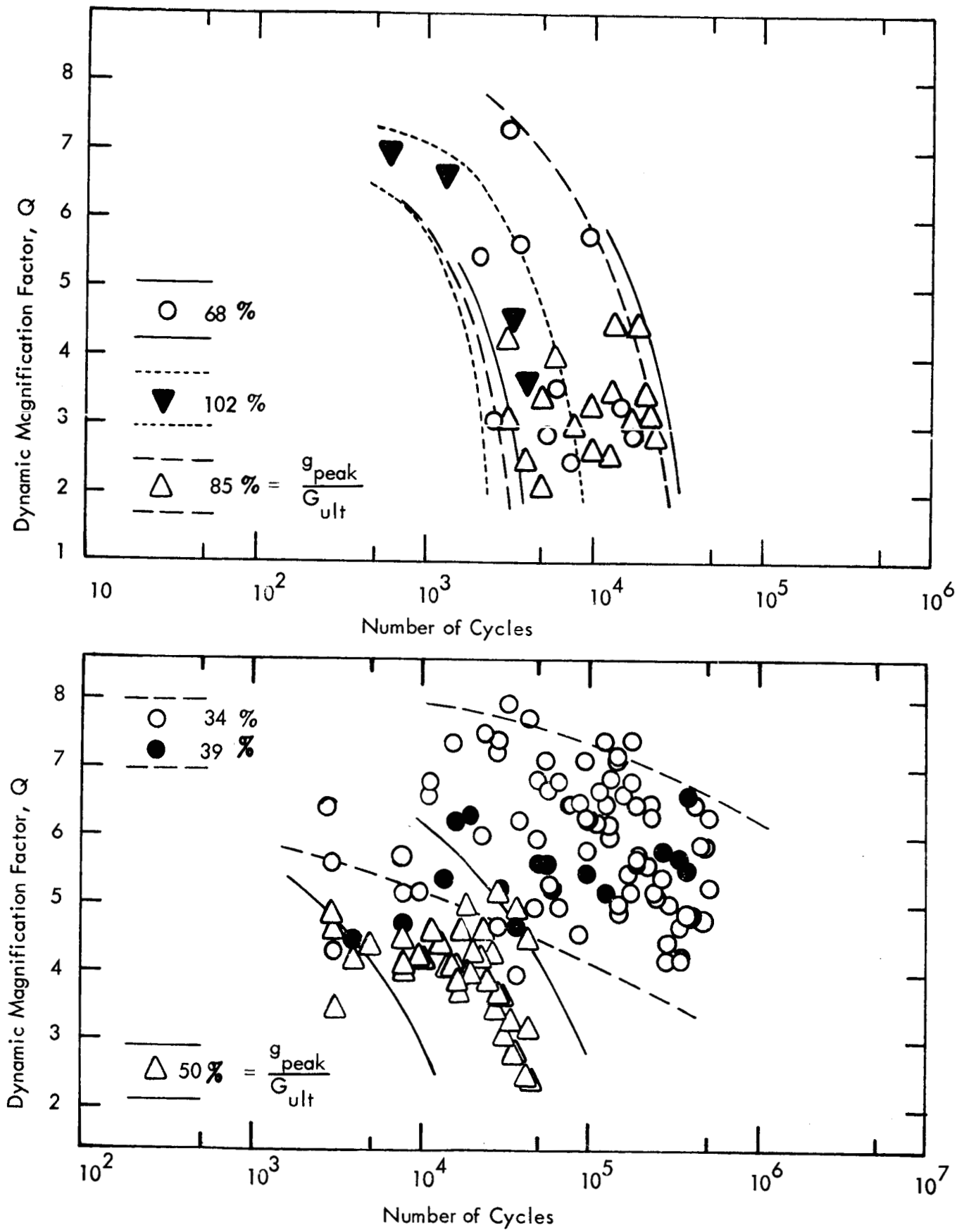

Figure 25. Variation of Dynamic Magnification Factor, Q, of Reinforced Concrete Subjected to Random Vibration.

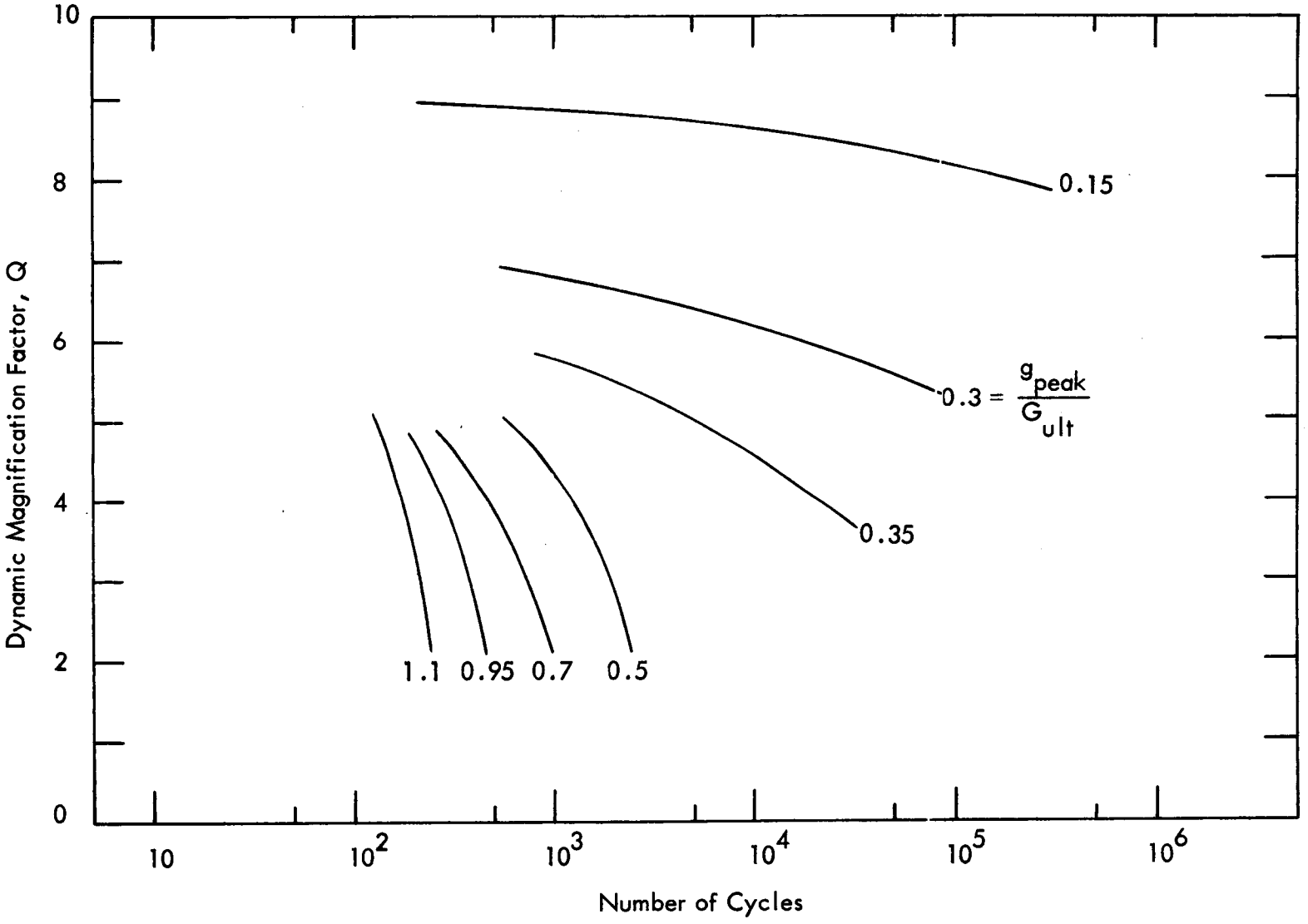

Figure 26. Synopsis of the Variations of the Dynamic Magnification Factor, Q, of Reinforced Concrete under Random Vibration from Figures 23, 24, and 25.

APPENDIX A

Calculations of Bending Moment, Area Moment of Inertia, and Fundamental Natural Frequency of the Scaled, Tensile Reinforced Concrete Beams

A. Double Reinforced Concrete

Dimension | Force Diagram | Strain Diagram

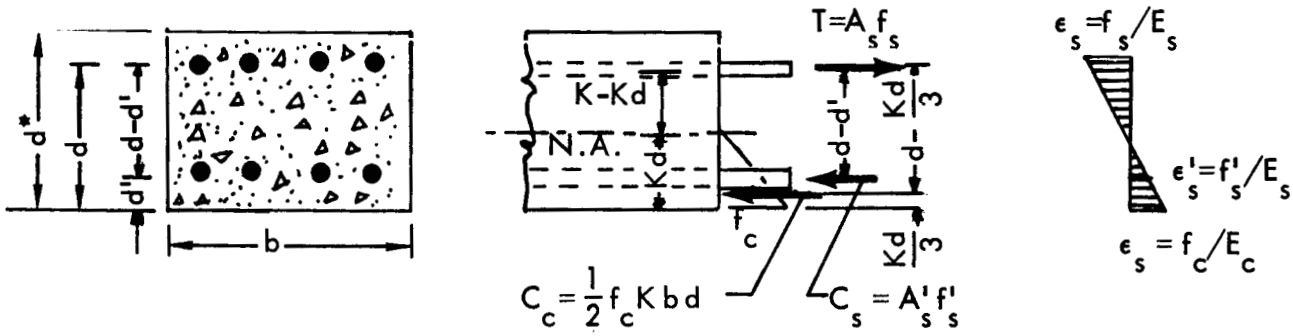

A_s = area of tensile steel

A'_s = area of compressive steel

A_c = area of compressive concrete

b = width of beam

d = depth of member from compression face to the centroid of the tensile steel

d' = distance from concrete face to centroid of steel

d^* = actual depth of beam

E_s = Young's modulus of elasticity of steel

E_c = Young's modulus of elasticity of concrete

f_s = stress in longitudinal tensile steel

f'_s = stress in longitudinal compressive steel

f_c = stress in longitudinal compressive concrete outer fiber

k = distance from compression face to the computed position of the neutral axis relative to depth d

n = $E_s/E_c = 30 \times 10^6/2 \times 10^6 = 15$

M = bending moment

p = A_s/b_d

p' = A'_s/bd

T = total tension force in steel

C_s = total compression force in steel

C_c = total compression force in concrete

ϵ_s = tensile strain of steel

ϵ'_s = compressive strain of steel

ϵ_c = compressive strain of concrete

Force Relationship:

$$T = A_s f_s = f_s \; p \; b \; d \qquad (1)$$

$$C = C_s + C_c = A'_s f'_s + \frac{1}{2} f_c \; k \; b \; d$$

$$= f'_s p' \; b \; d + \frac{1}{2} f_c \; k \; b \; d \quad . \qquad (2)$$

Taking $\Sigma F_{horiz.} = 0$, we get $T = C$, or

$$f_s p = f'_s p' + \frac{1}{2} f_c \; k \quad . \qquad (3)$$

Strains Relationship:

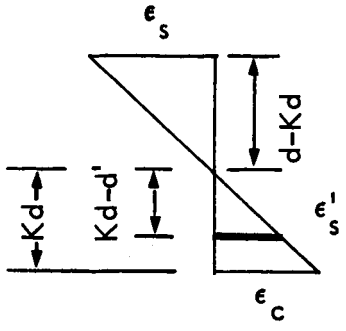

$$\frac{\text{Strain in Outer Compressive Concrete Fiber}}{\text{Strain in Tensile Steel}} = \frac{f_c/E_c}{f_s/E_s} = \frac{n f_c}{f_s} = \frac{k d}{d - k d} = \frac{k}{1 - k}$$

or $$f_s = n \frac{(1-k)}{k} f_c \quad . \qquad (4)$$

$$\frac{\text{Strain in Compressive Steel}}{\text{Strain in Tensile Steel}} = \frac{f_s'/E_s}{f_s/E_s} = \frac{f_s'}{f_s} = \frac{k d - d'}{d - k d}$$

or $$f_s' = f_s \frac{(k d - d')}{d(1-k)} \qquad (5A)$$

$$= n \frac{(1 - k)}{k} f_c \cdot \frac{(kd - d')}{d(1 - k)}$$

$$= n \frac{kd - d'}{kd} \cdot f_c \quad . \qquad (5B)$$

Substituting equations (4) and (5B) into (3), we get

$$n p \frac{(1-k)}{k} f_c = n p' \frac{kd - d'}{kd} f_c + \frac{1}{2} f_c k$$

$$n p (1 - k) = n p'(k - \frac{d'}{d}) + \frac{1}{2} k^2$$

$$(n p) - (n p) k = (n p') k - (n p' \frac{d'}{d}) + \frac{1}{2} k^2$$

$$(np) + np'\left(\frac{d'}{d}\right) - (np + np')k - \frac{1}{2}k^2 = 0$$

$$k^2 + 2(np + np')k - 2np - 2np'\left(\frac{d'}{d}\right) = 0 \cdot \qquad (6)$$

In general, $p = p'$, equation (6) becomes:

$$k^2 + (4np)k - 2np\left(\frac{d^*}{d}\right) = 0$$

$$k = \frac{-4np \pm \sqrt{(4np)^2 + 8np\left(\frac{d^*}{d}\right)}}{2}$$

$$k = \sqrt{(2np)^2 + (2np)(d^*/d)} - (2np) \cdot \qquad (7)$$

Note that equation (7) gives the position of the neutral axis. Taking the moment about the centroid of tensile steel, we have

$$M = \frac{1}{2} f_c k b d \left(d - \frac{kd}{3}\right) + f'_s A'_s (d - d')$$

$$= \frac{1}{2} f_c k b d \cdot d \left(1 - \frac{k}{3}\right) + n \frac{kd - d'}{kd} f_c \cdot p' b d \cdot (d - d')$$

$$= f_c b d \left[\frac{kd}{2}\left(1 - \frac{k}{3}\right) + n \frac{kd - d'}{kd} p' (d - d')\right] \cdot$$

$$f_c = \frac{M}{bd\left[\frac{kd(3-k)}{6} + \frac{n(kd - d')p'(d - d')}{kd}\right]}$$

$$= \frac{6kM}{b(kd)^2(3-k) + 6bn(kd - d')p'(d - d')} \cdot \qquad (8)$$

Thus

$$f_s = \frac{n(1-k)}{k} f_c$$

$$= \frac{6\,n\,(1-k)\;M}{b\,(kd)^2\,(3-k) \;+\; 6\,b\,n\,(kd-d')\,p'\,(d-d')} \quad . \qquad (9)$$

$$f'_s = \frac{n\left(\frac{kd-d'}{kd}\right) 6\,k\,M}{b\,(kd)^2\,(3-k) \;+\; 6\,b\,n\,(kd-d')\,p'\,(d-d')}$$

$$= \frac{6\,n\,(kd-d')\;M}{b\,d\,(kd)^2\,(3-k) \;+\; 6\,b\,d\,n\,(kd-d')\,p'\,(d-d')} \quad . \qquad (10)$$

If f_s is known from an experimental determination, a corresponding bending moment can be computed.

$$M = \frac{f_s\left[b\,(kd)^2\,(3-k) \;+\; 6\,b\,n\,(kd-d')\,p'\,(d-d')\right]}{6\,n\,(1-k)} \quad . \qquad (11)$$

For Model Concrete Beams :

f_s = 67.9 ksi (steel wires used in model concrete beam)

d' = 0.25 in.

d^* = 1.5 in.

d = 1.25 in.

n = E_s/E_c = 15

p = p' = 0.72 = 7.2×10^{-3}

f_s = 67.9 ksi

b = 3.5 in.

d^*/d = 1.2

np = 0.108

$2np$ = 0.216

$$(2np)^2 = 0.0466$$

$$(2np)\,(d^*/d) = 0.259$$

$$k = \sqrt{(2np)^2 + (2np)\,(d^*/d)} - 2np$$

$$= \sqrt{0.0466 + 0.259} - 0.216 = \sqrt{0.3056} - 0.216$$

$$= 0.553 - 0.216 = 0.337$$

$$kd = 0.337 \times 1.25 = 0.421 \text{ in.}$$

$$(kd)^2 = 0.177$$

$$(3 - k) = 3 - 0.337 = 2.663$$

$$(kd - d') = 0.421 - 0.25 = 0.171$$

$$(d - d') = 1.25 - 0.25 = 1.0$$

$$(1 - k) = 1 - 0.337 = 0.663 \ .$$

Using equation (11), we get,

$$M = \frac{f_s \left[b\,(kd)^2\,(3 - k) + 6\,b\,n\,(kd - d')\,p'\,(d - d') \right]}{6\,n\,(1 - k)}$$

$$= \frac{67.9 \times 10^3 \left[3.5\,(0.177)\,(2.663) + 6 \times 3.5 \times 15\,(0.171)\,7.2 \times 10^{-3}\,(1.0) \right]}{6 \times 15\,(0.663)}$$

$$= \frac{67.9 \times 10^3 \left[1.652 + 388 \times 10^{-3} \right]}{90\,(0.663)}$$

$$= \frac{67.9 \times 10^3 \left[2.040 \right]}{59.7}$$

$$= 2.32 \times 10^3$$

$$= 2320 \text{ in.} - \text{lb.}$$

From the actual static loading of beam, the average failing load, P, was 583 lbs. Therefore, the actual maximum bending moment is

$$M_{max} = \frac{1}{4} P (L - a) = \frac{1}{4} P (23.5 - 4) = \frac{1}{4} (19.5) P$$

$$= 4.9 P$$

$$= 4.9 \times 583 = 2850 \text{ in.} - \text{lb.}$$

The theoretical moment based on static ultimate strength of steel from axial loading conditions is fairly close to that from actual testing. The small discrepancy probably derives from the sources such as plastic deformation and big deflection of beam specimen at loads causing stresses greater than the material yield point.

B. The Area Moment of Inertia

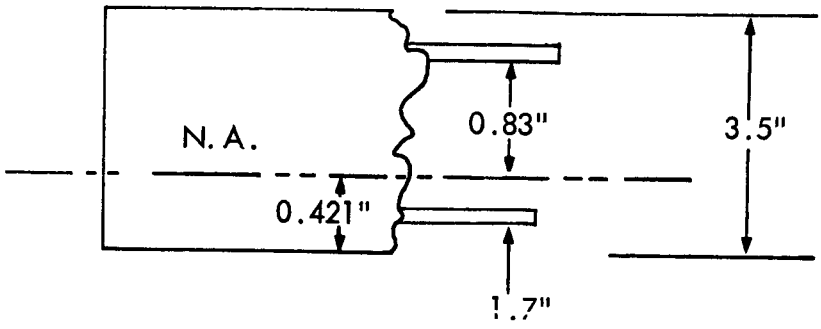

The area moment of inertia of the scale beam is:

$$I = \sum \left[\frac{b h^3}{12} + d^2 A \right]$$

$$= \left[\frac{3.5 \times 0.42^3}{12} + \left(\frac{0.42}{2} \right)^2 (3.5 \times 0.42) \right] +$$

$$\left[0 + (n p' b d)(0.17)^2 \right] + \left[0 + (n p' bd)(0.83)^2 \right]$$

$$= 0.0216 + 0.0646 + (15 \times 7.2 \times 10^{-3} \times 3.5 \times 1.25)(0.17^2 \times 0.83^2)$$

$$= 0.0216 + 0.0646 + 0.473 \times 0.719$$

$$= 0.426 \text{ in.}^4$$

C. Fundamental Natural Frequency:

The scale concrete beam possesses the following engineering constants:

Length: 23.5 inches between supports

Width: 3.5 inches

Depth: 1.5 inches

Young's Modulus of elasticity, $E = 2.5 \times 10^6$ psi

Area moment of inertia, $I = 0.426$ in.^{4}

Density: 150 lb./cu.ft.

Weight per unit length, $\mu = 0.503$ lb./in.

For pinned-pinned end fixity, the fundamental natural frequency is:

$$f_1 = \frac{1}{2\pi}\left(\frac{\pi}{L}\right)^2 \sqrt{\frac{g E I}{\mu}}$$

$$= \left(\frac{\pi}{2}\right)\left(\frac{1}{23.5}\right)^2 \sqrt{\frac{386 \times 2.5 \times 10^6 \times 0.426}{0.503}}$$

$$= 81.4 \text{ cps}.$$

APPENDIX B

Vibration of a Beam on Moving Supports

The equation of motion of a beam with moving supports can be expressed in terms of the absolute motion, $Y(x,t)$ of the beam or in terms of the sum of the support motion $U(t)$ and the relative deflection, $W(x, t)$ of the beam. Thus, if the bending stiffness is EI, the mass per unit length is ρA, and $Y(x,t) = U(t) + W(x,t)$, we can write the equation of motion as

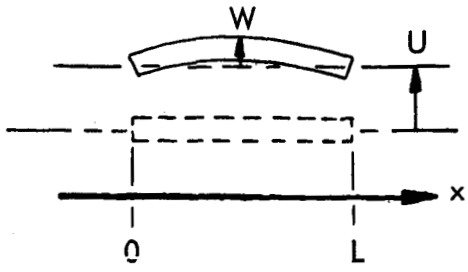

$$EI\frac{\partial^4 Y}{\partial x^4} + \rho A\frac{\partial^2 Y}{\partial t^2} = 0 \qquad 1)$$

or as

$$EI\frac{\partial^4 Y}{\partial x^4} + \rho A\frac{\partial^2 (U+W)}{\partial t^2} = 0 \cdot \qquad 2)$$

However,

$$\frac{\partial^4 Y}{\partial x^4} = \frac{\partial^4 W}{\partial x^4}, \text{ since } \frac{\partial^4 U}{\partial x^4} = 0$$

if the support motion U is the same at each end.

Thus, equation 2) becomes

$$EI\frac{\partial^4 W}{\partial x^4} + \rho A\frac{\partial^2 W}{\partial t^2} = -\rho A\frac{\partial^2 U}{\partial t^2} \cdot \qquad 3)$$

Two distinctly different forms of the solution to the problem are obtained depending on whether equation 1) or equation 3) is used. Briefly, use of equation 1) yields a closed form solution without expansion by the normal modes. This is due to the fact that two of the boundary conditions for this formulation specify non-zero conditions at the ends. The characteristic equations satisfying the boundary conditions are therefore not all homogeneous. Thus, the usual method of defining normal mode frequencies by setting the determinant of these equations equal to zero can not be used. With equation 3), on the other hand, the solution is carried out in the usual manner for forced vibration and results in a series solution expressing the motion as the net summation of vibration in the normal modes.

Although either method will produce equivalent results, the closed solution method has an advantage for simple computer calculation of the beam motion at any frequency.

Therefore, using equation 1), we assume the deflection Y takes the form:

$$Y(x,t) = Y(x) \sin \omega t$$

where ω is the frequency of excitation at the supports.

Thus $\frac{\partial^4 Y(x,t)}{\partial x^4} = Y''''(x) \sin \omega t$,

and $\frac{\partial^2 Y}{\partial t^2} = -\omega^2 Y(x) \sin \omega t$.

Substituting the above quantities into 1), we get

$$Y''''(x) \sin \omega t - \frac{\rho A}{E I} \omega^2 Y(x) \sin \omega t = 0$$

or $$Y''''(x) - K^4 Y(x) = 0 \qquad 4)$$

where $K^4 = \frac{\rho A}{E I} \omega^2$

or $$K^4 = \left(\frac{\pi}{L}\right)^4 \frac{\omega^2}{\omega_1^2} \qquad 5)$$

where $\omega_1^2 = \left(\frac{\pi}{L}\right)^4 \frac{E I}{\rho A}$, the fundamental frequency of a pinned-pinned beam.

The general solution of 4) is

$$Y(x) = A \cosh Kx + B \sinh Kx + C \cos Kx + D \sin Kx$$

where A, B, C and D are arbitrary constants.

Applying the boundary conditions:

$$Y(0) = Y(L) = U$$
$$Y''(0) = Y''(L) = 0,$$

we get, after a few mathematical manipulations,

$$A = C = \frac{U}{2}$$
$$B = -\frac{U}{2} \tanh \frac{KL}{2}$$
$$D = \frac{U}{2} \tan \frac{KL}{2} .$$

Thus,

$$Y(x) = \frac{U}{2}\left[\cosh Kx - \tanh \frac{KL}{2} \sinh Kx + \cos Kx + \tan \frac{KL}{2} \sin Kx\right] . 6)$$

For $KL = n\pi$, $n = 1, 3, 5,$ the last term goes to infinity. This corresponds to the odd-order resonant frequencies of the simply supported beam since, from equation 5)

$$\omega_n = K^2 \frac{EI}{\rho A} = \left(\frac{n\pi}{L}\right)^2 \frac{EI}{\rho A} .$$

Note that this shows that even-order modes are not excited by this symmetrical motion.

To introduce damping, we let E become complex with a loss tangent η. This will change K to a complex number which, for small η becomes:

$$K^* = K - j \frac{\eta}{4} K$$

where K = undamped wave number
η = the loss factor $\cong 1/Q$.

Then equation 6) becomes

$$Y(x) = \frac{U}{2}\left[\cosh\left(1 - j\frac{\eta}{4}\right)Kx - \tanh\left(1 - j\frac{\eta}{4}\right)\frac{KL}{2} \sinh\left(1 - j\frac{\eta}{4}\right)Kx + \cos\left(1 - j\frac{\eta}{4}\right)Kx + \tan\left(1 - j\frac{\eta}{4}\right)\frac{KL}{2} \sin\left(1 - j\frac{\eta}{4}\right)kx\right] ,$$

or expanding these functions into their real and imaginary terms,

$$Y(x) = a + j\,b \tag{7a}$$

$$\begin{aligned} \text{where } a = \frac{U}{2}\Bigg[& \cosh Kx \cos\left(\tfrac{\eta}{4} Kx\right) + \cos Kx \cosh\left(\tfrac{\eta}{4} Kx\right) \\ & + \frac{\sin KL}{\cos KL + \cosh\left(\tfrac{\eta}{4} KL\right)} \sin Kx \cosh\left(\tfrac{\eta}{4} Kx\right) \\ & - \frac{\sinh\left(\tfrac{\eta}{4} KL\right)}{\cos KL + \cosh\left(\tfrac{\eta}{4} KL\right)} \cos Kx \sinh\left(\tfrac{\eta}{4} Kx\right) \\ & - \frac{\sinh KL}{\cosh KL + \cos\left(\tfrac{\eta}{4} KL\right)} \sinh Kx \cos\left(\tfrac{\eta}{4} Kx\right) \\ & + \frac{\sin\left(\tfrac{\eta}{4} KL\right)}{\cosh KL + \cos\left(\tfrac{\eta}{4} KL\right)} \cosh Kx \sin\left(\tfrac{\eta}{4} Kx\right)\Bigg] \end{aligned} \tag{7b}$$

$$\begin{aligned} b = \frac{U}{2}\Bigg[& \sin Kx \sinh\left(\tfrac{\eta}{4} Kx\right) - \sinh Kx \sin\left(\tfrac{\eta}{4} Kx\right) \\ & - \frac{\sinh\left(\tfrac{\eta}{4} KL\right)}{\cos KL + \cosh\left(\tfrac{\eta}{4} KL\right)} \sin Kx \cosh\left(\tfrac{\eta}{4} Kx\right) \\ & - \frac{\sin KL}{\cos KL + \cosh\left(\tfrac{\eta}{4} KL\right)} \cos Kx \sinh\left(\tfrac{\eta}{4} Kx\right) \\ & + \frac{\sin\left(\tfrac{\eta}{4} KL\right)}{\cosh KL + \cos\left(\tfrac{\eta}{4} KL\right)} \sinh Kx \cos\left(\tfrac{\eta}{4} Kx\right) \\ & + \frac{\sinh KL}{\cosh KL + \cos\left(\tfrac{\eta}{4} KL\right)} \cosh Kx \sin\left(\tfrac{\eta}{4} Kx\right)\Bigg] \end{aligned} \tag{7c}$$

The magnitude of the absolute motion is

$$|Y(x)| = (a^2 + b^2)^{1/2} . \qquad 7d)$$

The magnitude of the relative motion is

$$|W(x)| = \left[(a - U)^2 + b^2\right]^{1/2} . \qquad 8)$$

Equation 8) has been evaluated for $\eta = 0.01$ and 0.125 loss factors typical for a lightly damped metal beam and a reinforced concrete bean, respectively. The mode shape, normalized to unit maximum deflection, is shown in Figure B1 for several frequencies. The frequency response of the maximum absolute deflection and phase at the middle of the beam relative to the applied motion is shown in Figure B2.

A simpler form of equation 7a) through 7d), to define the approximate response at the middle of the beam at resonance, is obtained by using only the last term in equation 6). With a complex molulus in the tan K L term only, the resonant response at $x = L/2$ is given approximately by

$$Y_{max} \simeq \frac{U_s}{2} \left[-j \frac{\sinh \frac{\eta}{4} KL \sin \frac{KL}{2}}{\cos KL + \cosh \frac{\eta}{4} KL} \right] .$$

For low damping and $KL = m\pi$, $m = 1, 3, 5$ etc., a series expansion reduces this to a simpler approximation which is the same as the maximum relative displacement found by a normal mode solution

$$Y_{max} \simeq U \left[-j (4/\eta \; n\pi) \right] \left[-1 \right]^{(n-1)/2} , \quad n = 1, 3, 5, \text{ etc.} \qquad 9)$$

The maximum response predicted by equation 9) is also shown on Figure B2.

The variation in stress along the beam is determined exactly by taking the second derivative of the mode shape in equation 7a) through 7d). The bending stress is then:

$$\sigma = E C Y''(x)$$

where C = distance from centroidal axis to outer most "fiber"
E = modulus of elasticity.

The second derivative, Y'', of equation 7a) through 7d) is not shown here for the sake of brevity. Numerical values were determined however by the computer program mentioned earlier. The results of this analysis was applied to the vibration fatigue tests of pinned-pinned concrete beam specimens.

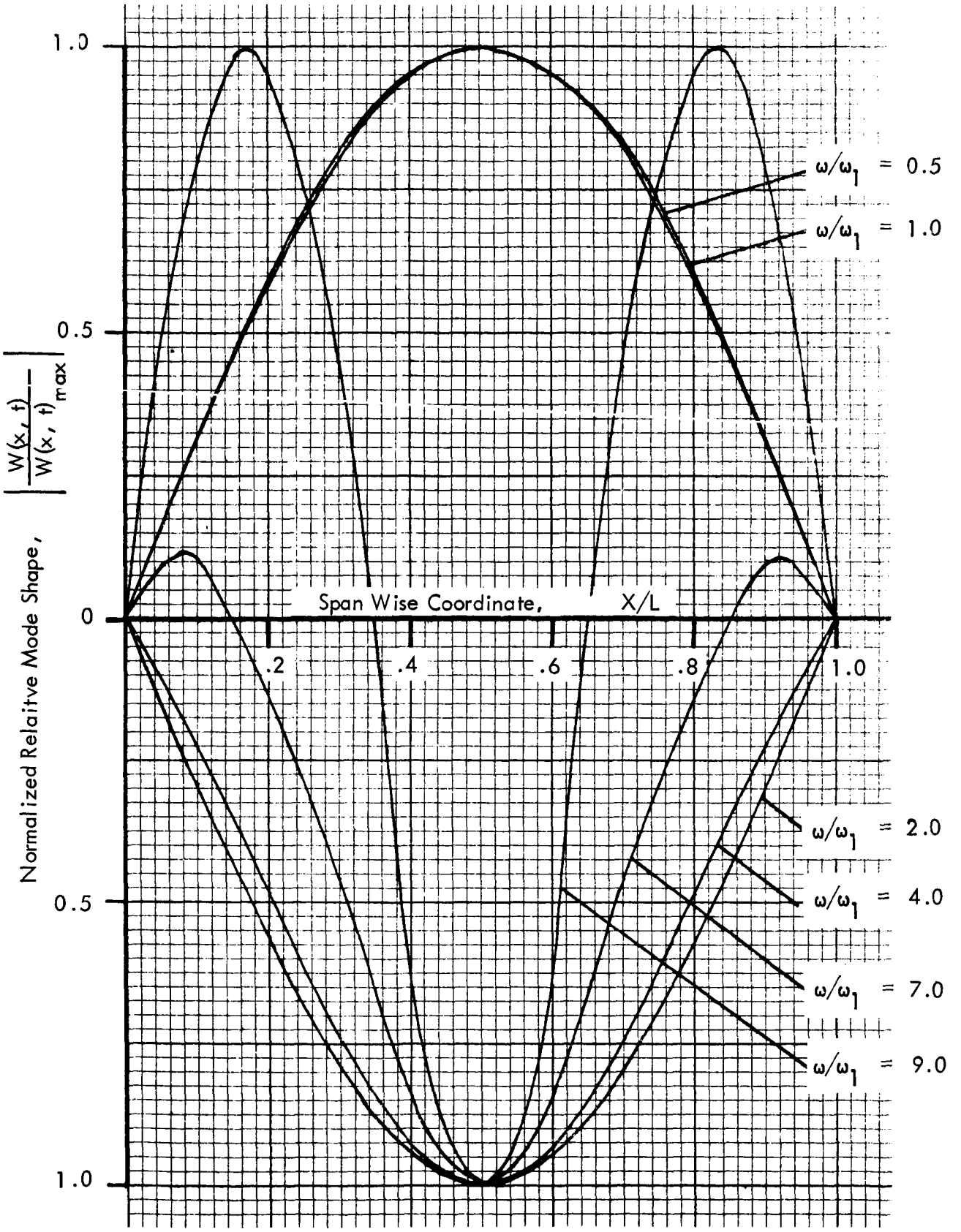

Figure B1. Normalized Relative Mode Shape $W(x, t)/W(x, t)_{max}$ with Loss Factor $\eta = 0.125$.

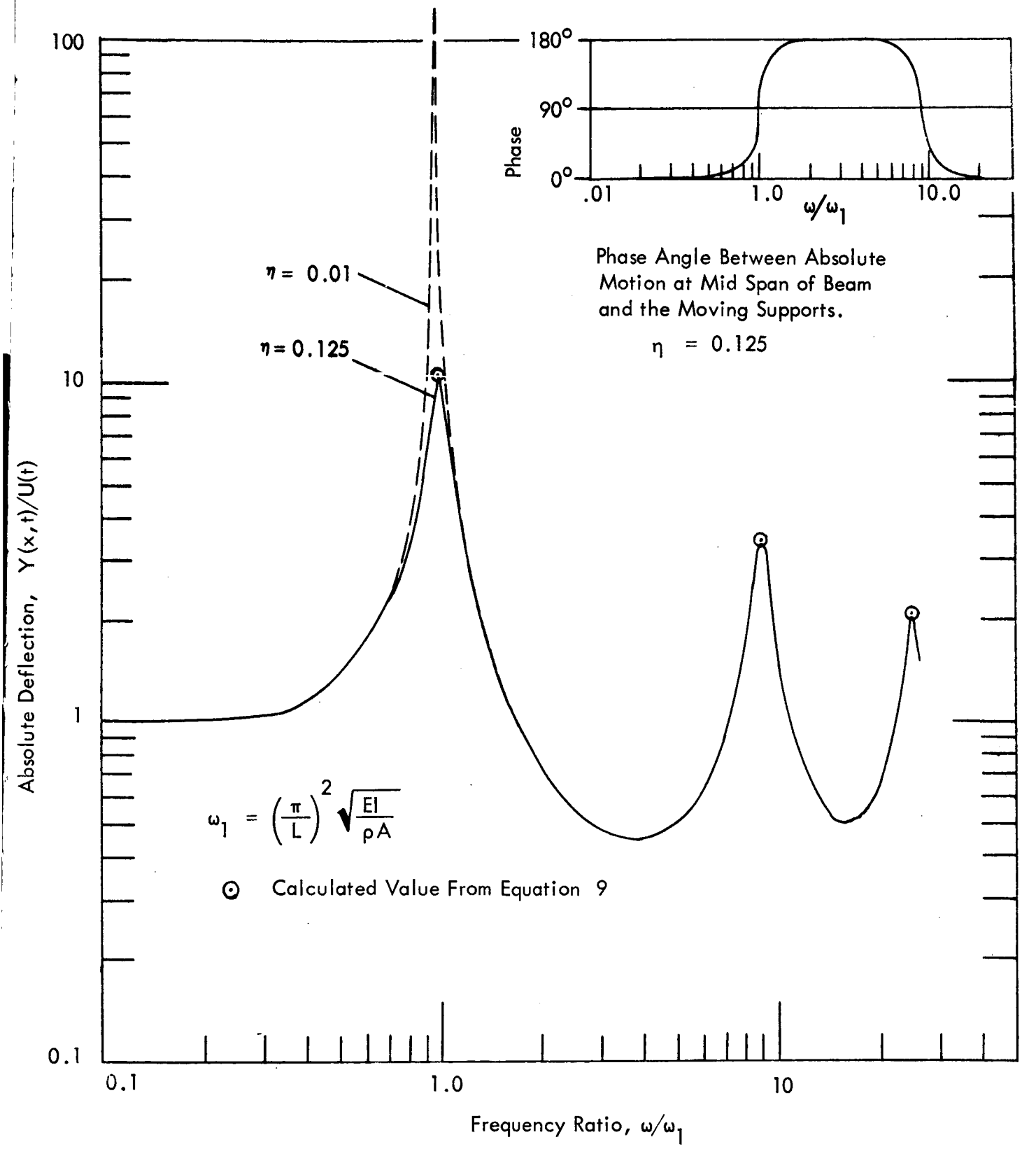

Figure B2. Absolute Deflection $Y(x,t)$ at Mid Span of a Simply Supported Beam ($X/L = 0.5$) With Moving Supports and Loss Factor η.

APPENDIX C

Illustrations of Fatigue Failure Estimation of Reinforced Concrete Under Random Loading

Example 1

Estimate the fatigue life of a simply supported reinforced concrete beam, 12 in. x 6 in. x 15 ft., subjected to random acoustic normal excitation. The maximum spectral density of acceleration response is measured at midspan to be 8 g^2/cps. Ultimate strength of the beam is assumed to be 4000 psi, and $Q = 8$.

Calculations:

$$E I = 2.5 \times 10^6 \times \frac{12 \times 6^3}{12} = 5.4 \times 10^8 \text{ lb. in.}^2$$

$$\mu = 0.096 \text{ lb./in.}^3 = 0.096 \times 12 \times 6 = 6.91 \text{ lb./in.}$$

$$f_1 = \frac{1}{2\pi} \left(\frac{\alpha_1}{L}\right)^2 \sqrt{\frac{g E I}{\mu}}$$

where α_1 = frequency parameter

= π for simply supported beam .

$$f_1 = \frac{1}{2\pi} \left(\frac{\pi}{180}\right)^2 \sqrt{\frac{386 \times 5.4 \times 10^8}{6.91}}$$

= 8.4 cps .

$$G_{ult} = \frac{4 f_1^2 L^2}{E c g} \sigma_{ult}$$

$$= \frac{4 \times 8.4^2 \times 180^2}{2.5 \times 10^6 \times 3 \times 386} \times 4000 = 12.6 \, g_{peak} .$$

$$g_{rms} = \left[\frac{\pi}{2} \; S_{\ddot{W}}(\omega_1) \; \frac{f_1}{Q} \right]^{1/2}$$

$$= \left[\frac{\pi}{2} \; (8) \; \frac{8.4}{8} \right]^{1/2}$$

$$= 3.64 \; g \; .$$

Assume that $g_{peak} = 3 \times g_{rms}$,

$$g_{peak} = 3 \times 3.64 = 10.9 \; g \; .$$

$$\frac{g_{peak}}{G_{ult}} = \frac{10.9}{12.6} = 0.865 \; .$$

From Figure 22, the fatigue life of the beam is between 1,200 to 20,000 cycles; or 190 to 3,180 seconds, assuming that the resonance frequency drops to half of its initial value at time of specimen failure.

Example 2

Same beam as in Example 1 except clamped at both ends. Maximum acceleration spectral density at midspan is 1.5 g^2/cps. Again, σ_{ult} = 4000 psi, and Q = 8.

From statics we know that the bending moment at the ends is twice that at the middle of the beam. We, therefore, assume that the maximum acceleration spectral density to be 6 g^2/cps.

$$f_1 = \frac{1}{2\pi} \left(\frac{\alpha_1}{L} \right)^2 \sqrt{\frac{g \, E \, I}{\mu}}$$

where α_1 = 4.730 for clamped-clamped beam .

$$f_1 = 19.1 \; \text{cps} \; .$$

The fundamental beam mode shape can be expressed as:

$$y(x, t) = y_c \left(1 - \cos \frac{2\pi x}{L}\right) e^{i\omega t} .$$

Differentiating with time twice we get,

$$\frac{\partial^2 y(x, t)}{\partial t^2} = \ddot{y}(x, t) = - \omega^2 y_c \left(1 - \cos \frac{2\pi x}{L}\right) e^{i\omega t}$$

$$= - \omega^2 \, y(x, t)$$

or

$$y(x, t) = - \frac{1}{\omega^2} \ddot{y}(x, t) .$$

Again, differentiating twice with spanwise coordinate x, we have:

$$\frac{\partial^2 y(x, t)}{\partial x^2} = 4 \left(\frac{\pi}{L}\right)^2 y_c \, e^{i\omega t} \cos \frac{2\pi x}{L} .$$

Let $x = 0$ or L, and ωt = multiple of 2π.

$$\left| \frac{\partial^2 y(x, t)}{\partial x^2} \right|_{max} = 4 \left(\frac{\pi}{L}\right)^2 y_c$$

$$= 4 \left(\frac{\pi}{L}\right)^2 y(x, t)_{max}$$

$$= 4 \left(\frac{\pi}{L}\right)^2 \frac{1}{\omega^2} \ddot{y}(x, t)_{max} .$$

The maximum bending moment can be shown as:

$$M_{max} = E I \left| \frac{\partial^2 y(x, t)}{\partial x^2} \right|_{max}$$

$$= E I \; 4\left(\frac{\pi}{L}\right)^2 \; \frac{1}{\omega^2} \; \ddot{y}(x, t)_{max}$$

$$= E I \; \frac{1}{L^2 f^2} \; \ddot{y}(x, t)_{max} .$$

$$\ddot{y}(x, t)_{max} = \frac{f^2 L^2}{E I} M_{max}$$

$$= \frac{f^2 L^2}{E c} \sigma_{max} .$$

Finally, we get,

$$G_{ult} = \frac{f^2 L^2}{E c g} \sigma_{ult}$$

$$= \frac{(19.1)^2 \; (180)^2}{2.5 \times 10^6 \times 3 \times 386} \times 4000$$

$$= 16.35 \; g_{peak} .$$

The response in terms of rms acceleration is 4.74 g_{rms}, and g_{peak} is 14.2 g.

Thus, we have

$$\frac{g_{peak}}{G_{ult}} = \frac{14.2}{16.35} = 0.87 .$$

From Figure 22, the fatigue life of the beam is between 1,000 to 18,000 cycles; or 74 to 1330 seconds, if we assume that the resonance frequency drops to half of its initial value at time of specimen failure.

Example 3

Same beam as Example 1 except the spectral density of acceleration response is recorded as 1 g^2/cps at time five minutes after the onset of the random acoustic excitation test. The dynamic magnification factor, Q, for a virgin specimen is assumed to be 8. Resonance frequency is 7.6 cps at time of recording.

The theoretical natural frequency of the virgin concrete beam specimen, from Example 1, is calculated as 8.4 cps. This frequency drops to a lower value due to the change of bending stiffeners, EI, which was a direct result of some macro- or micro - cracks in the concrete subjected to severe vibration. A frequency average of 8.0 cps is assumed for the first five minute period. The number of load cycles is:

$$N = 8.0 \times 5 \times 60 = 2{,}400 \text{ cycles.}$$

Now, we assume that at the onset of test, the ratio $\frac{g_{peak}}{G_{ult}}$ equals 0.35. From Figure 26, Q is approximately 5.8 at 2,400 cycles.

Since the excitation force is the same at onset of test and at time five minutes later, we have, from page 17,

$$\left[\frac{S_{\ddot{W}_1}(\omega_1)}{1.6\,Q^2}\right]_{\substack{\text{Onset}\\ \text{of test}}} \cong S_{\ddot{W}_o}(\omega_1) \cong \left[\frac{S_{\ddot{W}_1}(\omega_1)}{1.6\,Q^2}\right]_{5\text{ Minutes}}$$

or

$$\left[S_{\ddot{W}_1}(\omega_1)\right]_{\substack{\text{Onset}\\ \text{of test}}} = \left[\frac{Q_{\text{onset of test}}}{Q_{\text{5 minutes}}}\right]^2 \left[S_{\ddot{W}_1}(\omega_1)\right]_{5\text{ Minutes}}$$

$$= \left(\frac{8}{5.8}\right)^2 (1)$$

$$= 1.9 \quad g^2/\text{cps.}$$

At the onset of test, we have,

$$g_{peak} = 3 \times \left[\frac{\pi}{2} S_{\ddot{W}_1}(\omega_1) \frac{f_1}{Q} \right]^{1/2}$$

$$= 3 \times \left[\frac{\pi}{2} (1.9) \frac{8.4}{8} \right]^{1/2}$$

$$= 5.3 .$$

From Example 1, we have $G_{ult} = 12.6$, thus

$$\frac{g_{peak}}{G_{ult}} = \frac{5.3}{12.6} = 0.42 .$$

The initial assumption, $\frac{g_{peak}}{G_{ult}} = 0.35$, is not too far off.

From Figure 22, for $\frac{g_{peak}}{G_{ult}} = 0.42$, the life cycles are approximately 20,000 to 300,000; or, 3,180 to 47,700 seconds assuming that the resonance frequency drops to half if its initial value at time of specimen failure.

Example 4

A concrete beam, similar in dimensions and support conditions to that of Example 1, is reinforced by structural steel which runs parallel to the beamwise axis and is imbedded at the center of the concrete. At the beginning of a random vibration test, the response at the middle of the beam is 0.1 g^2/cps. Assume $\sigma_{ult,\ tension} = 400$ psi, $\sigma_{ult,\ compression} = 5000$ psi, and $Q = 8$.

The ultimate strength of the beams in the previous three examples was 4000 psi (tensile or compression, whichever was lower). This high strength indicated that the beams had their top and bottom surfaces reinforced by tensile steel.

In this final example, the beams may have the same amount of reinforcement as those in the previous examples. However, since the reinforcing steel is in the plane of the neutral axis of the beam, the tensile strength of the outermost fiber of the beam is not benefited from the steel. We shall, therefore, analyze this last beam, based only on its ultimate tensile strength. G_{ult} can be shown to be $1.26\, g_{peak}$.

f_1 is still 8.4 cps

g_{rms} is 0.406 g, and g_{peak} is 1.22 g.

The ratio g_{peak}/G_{ult} is 0.97.

The estimated life of the beam is between 400 to 6000 cycles.

The purpose of this example is clear. The position of the reinforcement is important when the specimen is subjected to a complex reverse loading process, such as sinusoidal or random vibrations. The percentage of reinforcement becomes of secondary importance. The beam in this last example would probably be severely cracked, but not necessarily completely broken, after the estimated vibration cycles.